EARTHQUAKE ACTIVITY AND GROUND SHAKING IN AND ALONG THE EASTERN GULF OF ALASKA

by

John C. Lahr and Christopher D. Stephens

Office of Earthquakes, Volcanoes, and Engineering
U.S. Geological Survey

Final Report
Outer Continental Shelf Environmental Assessment Program
Research Unit 210

1983

29

This study was supported by the Bureau of Land Management through interagency agreement with the National Oceanic and Atmospheric Administration, under which a multi-year program responding to needs of petroleum development of the Alaskan Continental Shelf is managed by the Outer Continental Shelf Environmental Assessment Program Office.

TABLE OF CONTENTS

LIST OF FIGURES

Figure 9a. Map of epicenters for 155 earthquakes that occurred between March 28, 1964 and April 12, 1964, the first two weeks following the 1964 Alaska earthquake. Symbols and labels same as Figure 6a.

Figure 9b. Epicenters during first two weeks following the 1964 earthquake, as in Figure 9a. The eastern boundary of the 1964 rupture zone, as defined by McCann and others (1979), is shown .

Figure 10a. Epicenter map of 453 earthquakes that occurred between April 13, 1964 and September 30, 1974. Symbols and labels same as Figure 6a.

Figure 10b. April 13, 1964 through September 30, 1974 epicenters, as in Figure lOa.

Figure 11. Plot of EDF body-wave magnitude (rob) versus coda magnitude calculated from local stations.

Figure 12a. Epicenter map of 42 earthquakes with coda magnitudes greater than or equal to 3.5 that occurred between October 1, 1974 and September 31, 1981. Labels same as Figure 6a. Note change in symbol values from previous figures.

Figure 12b. October 1, 1974 through September 30, 1981 epicenters, as in Figure 12a.

Figure 13a. Epicenter map of 2015 earthquakes located by the local seismograph network between October 1, 1974 and February 28, 1979 just prior to the St. Elias earthquake. Labels same as Figure 6a. Note that symbol values are larger than in previous figures.

Figure 13b. October 1, 1974 through February 28, 1979 epicenters, as in Figure 13a.

Figure 14a. Epicenter map of 287 earthquakes located by the local seismograph network starting with the St. Elias earthquake on February 28, 1979 through March 20, 1979. Labels same as Figure 6a.

Figure 14b. February 28, 1979 through March 20, 1979 epicenters, as in Figure 14a.

Figure 15. Epicenter map of 3534 earthquakes located by the local seismograph network between October 1, 1979 and September 30, 1980. Labels same as Figure 6a.

Figure 15b. October 1, 1979 through September 30, 1980 epicenters, as in Figure 15a.

LIST OF TABLES

I. SUMMARY OF OBJECTIVES, CONCLUSIONS, AND IMPLICATIONS WITH RESPECT TO OCS OIL AND GAS DEVELOPMENT

A. Objectives

The objective of this research has been to develop information necessary for improved assessment of the hazards posed by earthquakes to development of oil and gas within the northeast Gulf of Alaska (NEGOA) and adjacent onshore areas.

B. Conclusions

The NEGOA region lies along the boundary of the North American and Pacific lithospheric plates and is seismically active due to the relative motion of these plates. A kinematic model has been developed which specifies the slip rates on the principal faults that accommodate the relative plate motion, and this model allows an estimate to be made of the long-term rate of seismicity on each fault. Based on this model and on the theory of seismic gaps, the coastal zone between Icy Bay and Kayak island is thought to be a likely site for a magnitude 8 or larger earthquake within the next two or three decades. The model also suggests that infrequent great ($M_S > 8$) earthquakes could occur on the low-angle megathrust zone which is thought to underlie the entire continental shelf between Cross Sound and Kayak Island.

In addition to the hazard from infrequent great events, moderate and large-size earthquakes ($5.5 < M_S < 8$) could occur throughout the entire coastal zone and pose a more localized hazard. This type of event could occur along the underlying megathrust zone or on faults within either of the interacting lithospheric plates. The source regions for such events are not limited to areas that are currently experiencing relatively high rates of microearthquake activity.

C. Implications

The northeast Gulf of Alaska lies within an active tectonic region which will continue to be subjected to the effects of earthquakes. In addition to generating strong ground shaking, earthquakes could trigger tsunamis, seiches, submarine slumping, and surface faulting, any of which could be hazardous to offshore and coastal structures. Careful consideration must clearly be given to these potential seismic hazards in developing oil and gas resources within the northeast Gulf of Alaska.

II. INTRODUCTION

A. General nature and scope of study

The purpose of this research has been to investigate the earthquake potential in the NEGOA and adjacent onshore areas. This was accomplished by reviewing the historical seismic record as well as by collecting new and more detailed information on both the distribution of current seismicity and the nature of strong ground motion resulting from large earthquakes.

B. Specific objectives

1. Review historical record of earthquakes in the NEGOA.

2. Record the locations and magnitudes of all significant earthquakes within the NEGOA area.

3. Prepare focal mechanism solutions to aid in interpreting the tectonic processes active in the region.

4. Identify both offshore and onshore faults that are capable of generating earthquakes.

5. Assess the nature of strong ground shaking associated with large earthquakes in the NEGOA.

6. Evaluate the average recurrence time for large events within and adjacent to the NEGOA.

C. Relevance to the problem of petroleum development

It is crucial that the seismic potential in the NEGOA be carefully analyzed and that the results be incorporated into the plans for future petroleum development. This information should be considered in the selection of tracts for lease sales, in choosing the localities for oil pipelines and land-based operations, and in setting minimum design specifications for both coastal and offshore structures.

111. CURRENT STATE OF KNOWLEDGE

The current relative motions of the rigid plates that constitute the earth's outer shell (lithosphere) have been well-established based on many lines of geological and geophysical evidence, including the pattern of ocean-bottom magnetic anomalies, the orientation of major strike-slip faults, the global distribution of earthquakes, and earthquake focal mechanisms (see, for example, Minster and Jordan, 1978). The Aleutian trench, located south of the Aleutian arc and the Alaska Peninsula and extending as far east as the Gulf of Alaska, forms part of the near-surface expression of the Pacific-North American plate boundary. The boundary also follows the Queen Charlotte Islands fault along southeastern Alaska and Canada. The relative motion of these two plates results in SE-NW convergence along the Aleutian megathrust and right lateral strike-slip motion on the Queen Charlotte Islands fault (Figure 1). Direct evidence for this convergent motion today comes from studies of large earthquakes along sections of the Pacific-North American plate boundary adjacent to the NEGOA . For example, the 1964 Alaska earthquake resulted from low-angle, dip-slip motion of about 12 m (Hastie and Savage, 1970) on the section of the Aleutian megathrust extending from beneath eastern Prince William Sound to southern Kodiak Island. While the plate boundary in the source region of the 1964 earthquake and along the Queen Charlotte Islands fault is thought to be relatively simple. the precise manner in which the relative plate motion is accommodated in the intervening NEGOA region is still the subject of investigation. Accurate assessment of the seismic hazard in the NEGOA can only be made when the relative motion between the Pacific and North American plates can be understood in terms of the displacement rates on the faults that accommodate the motion. Toward this end, one of the principal results of this research has been the development of a working model for the kinematics of the NEGOA region.

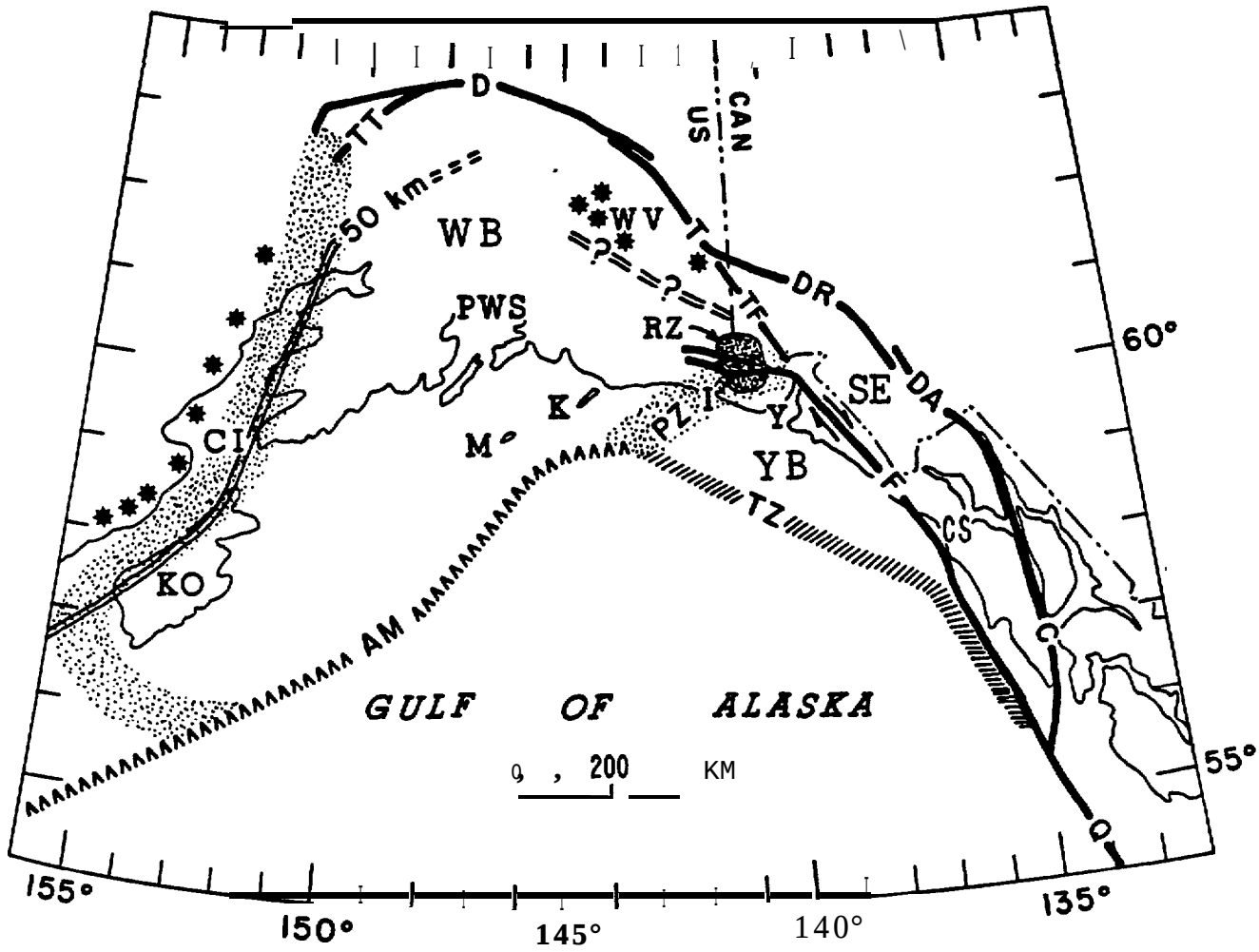

Figure 1. Map of southern Alaska and western Canada emphasizing the principal regional tectonic features. Faults after **Clague** (1979) and **Beikman** (1978). KO, Kodiak Island; M, Middleton Island; **K,** Kayak Island; **CI,** Cook Inlet; PWS, Prince William Sound; I, Icy Bay; Y, **Yakutat** Bay; CS, Cross **Sound; WV, Wrangell volcanics; RZ,** rupture zone of 28 February 1979 earthquake; AM, Aleutian **megathrust;** TZ, Transition zone; Q, Queen Charlotte Islands fault; C, **Chatham** Strait fault; DA, Dalton fault; DR, Duke River fault; TF, possible fault connecting the Fairweather and **Totschunda** faults; T, Totschunda fault; D, **Denali** fault; TT, unnamed faults; F, Fairweather fault; PZ, **Pamplona** zone; YB, **Yakutat** block; SE Saint **Elias** block; WE, **Wrangell** block; double line marks 50 **km** isobath of **Benioff** zone, queried where inferred; stippled bands mark surface outcrops of major zones of deformation and faulting.

IV. STUDY AREA

This project is concerned with the seismicity within and adjacent to the eastern Gulf of Alaska continental shelf. The area includes southern coastal Alaska and the adjacent continental shelf region between Prince William Sound and Yakutat.

V. METHODS AND RATIONALE OF DATA COLLECTION

A. High-gain, high-frequency seismograph network

The high-gain, high-frequency seismograph stations operated along the eastern Gulf of Alaska largely with funds from the Outer Continental Shelf Environmental Assessment Program are shown in Figure 2. Single-component stations record the vertical component of the ground motion, while three-component stations have instruments to measure north-south and east-west motions as well. The seismic signals detected by these instruments are transmitted by frequency-modulated radio and telephone links to a central recording facility in Palmer, Alaska, where they are photographically recorded on 16-mm film. The films are sent to Menlo Park, California for data processing and analysis.

Data from these instruments are used to determine the parameters of earthquakes as small as magnitude 1. The parameters of interest are origin time, epicenter, depth, magnitude, and for larger shocks, focal mechanism. These data are required to further our understanding of the regional tectonics, to identify active faults, and to assess rates of seismic activity.

B. Earthquake locations

Earthquakes of interest are selected by scanning the 16-mm films and noting times of occurrence. Timing is done by projecting the seismic traces onto a table such that 1 cm corresponds to 1 sec in time, and then digitizing x,y data pairs corresponding to P- and S-wave arrival times, duration of signal in excess of a given threshold, and period and amplitude of maximum signal. The directions of P-wave first motions are also noted. The digitized data are converted to phase data using the computer program DIGIT3 (written by P. L. Ward and W. L. Ellsworth, U.S.G.S., modified by C. D. Stephens), and then are processed using the program HYPOELLIPSE (Lahr, 1980) to determine hypocenter parameters. The P-wave velocity model used for the NEGOA region features a crust of linearly increasing velocity from 5 km/s at the surface to 7.8 km/s at 32 km depth overlying a half-space of 8.2 km/s. A constant P to S-velocity ratio of 1.78 is assumed.

Details of the operation of the high-gain, high-frequency seismograph network and the processing of the seismic data can be found in published catalogs (for example, Stephens and others, 1982).

C. Magnitude determination

Magnitudes are determined from the maximum trace amplitude or the signal duration. Eaton and others (1970) approximate the Richter local magnitude, which by definition is derived from maximum trace amplitudes recorded on

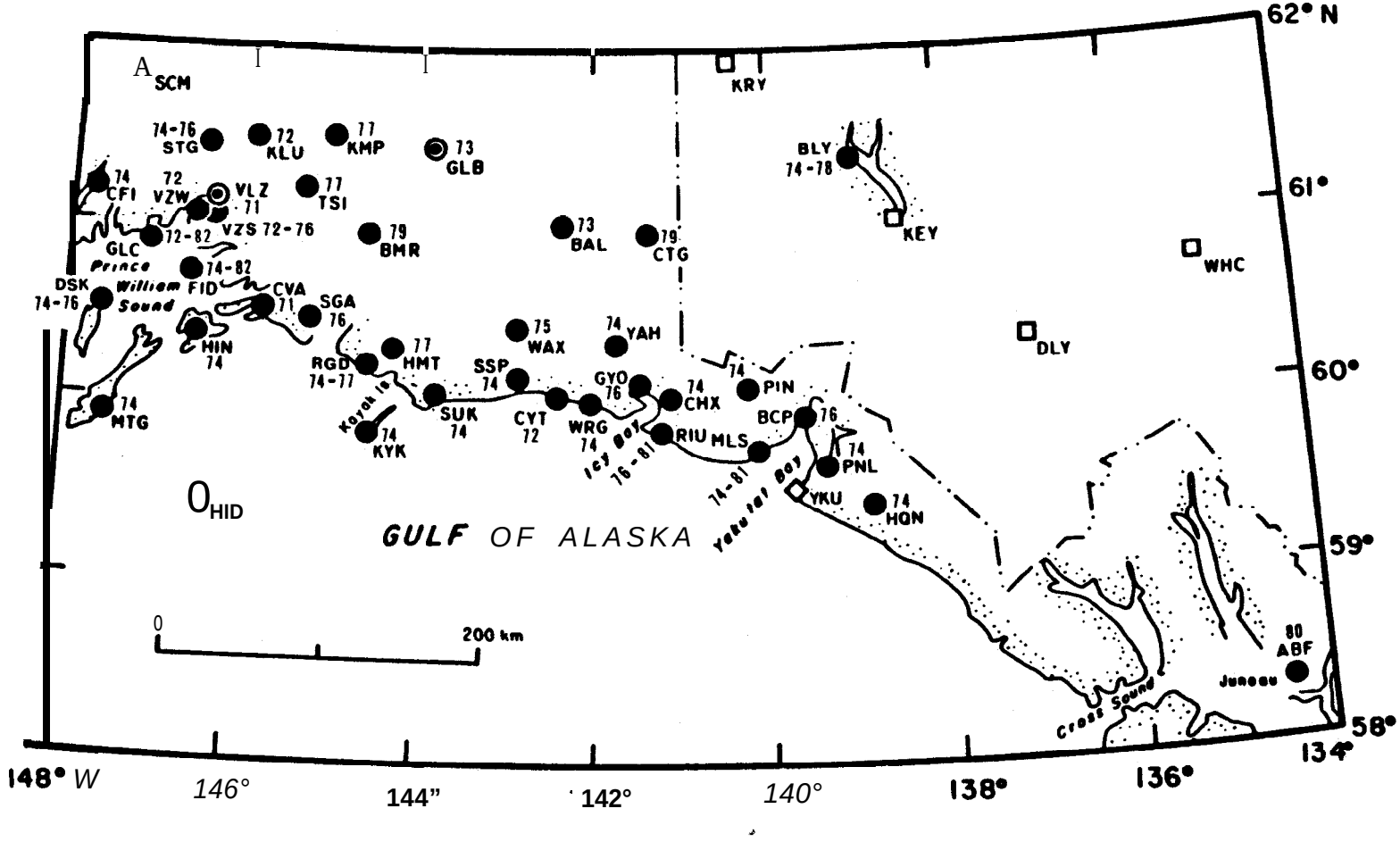

Figure 2. High-gain vertical-component seismic **stations operated In the** NEGOA and adjacent areas during 1974 through **1981.** The symbols are as follows: **solid** circles--USGS vertical stations; circles with center dot--USGS three-component stations; diamonds--Alaska Tsunami Warning Center stations; triangle--University of Alaska station; **squares--stations** operated by the Canadian Department of Energy, Mines and Resources. The station at Middleton Island (MID) was not operational between March 1979 and February 1981. For the USGS stations the year(s) of installation (and removal) is given. The stations installed in 1974-1976 were purchsed with OCSEAP funds.

standard horizontal Wood-Anderson torsion seismographs, by an amplitude magnitude based on maximum trace amplitudes recorded on high-gain, high-frequency vertical seismographs such as those operated in the Alaskan network. The amplitude magnitude, XMAG, used is based on the work of Eaton and his co-workers and is given by the expression (Lee and Lahr, 1972):

$$XMAG = \log_{10}A - B_1 + B_2 \log_{10}D^2 \quad (1)$$

where A is the equivalent maximum trace amplitude in millimeters on a standard Wood-Anderson seismograph, D is the hypocentral distance in kilometers and B_1 and B_2 are constants. Differences in the frequency response of the seismograph systems are accounted for in calculating A. It is assumed, however, that there is no systematic difference between the maximum horizontal ground motion and the maximum vertical motion. The terms $-B_1 + B2 \log_{10}D^2$ are normalizing terms and equal the logarithm of the trace amplitude for an earthquake of magnitude zero as a function of epicentral distance D. The constants are: B_1 = 0.15 and B2 = 0.08 for D = 1 to 200 km and B_1 = 3.38 and B_2 = 1.50 for D = 200 to 600 km.

Due to the limited dynamic range of the film recordings the maximum trace amplitude is often offscale. To circumvent this problem, coda duration is also used to estimate the magnitude. For small, shallow earthquakes in central California, Lee and others (1972) express the coda duration magnitude FMAG at a given station by the relationship

$$FMAG = -0.87 + 2.0 \log_{10}T + 0.0035\ D \quad (2)$$

where T is the signal duration in seconds from the P-wave onset to the point where the peak-to-peak trace amplitude on the Geotech Model 6585 film viewer with 20X magnification falls below 1 cm, and D is the epicentral distance in kilometers.

Comparison of XMAG and FMAG estimates from equations (1) and (2) for 77 Alaskan shocks in the Cook Inlet region in the depth range O to 150 km and in the magnitude range 1.5 to 3.5 reveals a systematic linear decrease of FMAG relative to XMAG with increasing focal depth. Also, Alaskan earthquakes show no systematic dependence of T on D. The following equation is therefore used, including a linear depth-dependence term, but no distance term:

$$FMAG = -1.15 + 2.0 \log_{10}T + 0.007\ Z \quad (3)$$

where Z is the focal depth in kilometers.

The magnitude preferentially assigned to each earthquake is the mean of the FMAG (equation 3) estimates obtained for USGS stations. The XMAG estimate is used when no FMAG determination can be made.

D. Strong-motion network

Strong-motion instruments are designed to trigger during large earthquakes and give high quality records of large ground motions which are

necessary for engineering design purposes. This type of instrument was first installed in Alaska following the 1964 Alaska earthquake. Between 1974 and 1981 OCSEAP funding supported both the installation and maintenance of additional strong-motion instruments in southern Alaska. Figure 3 shows the locations of instruments, almost exclusively Kinemetrics SMA-1 accelerographs, operated by the USGS and their dates of installation and removal.

VI. RESULTS AND DISCUSSION

A. Proposed kinematic model for Pacific-North American interaction

A working model has been developed for the Holocene Pacific-North American plate interaction along the Gulf of Alaska (Lahr and Plafker, 1980). In this model deformation within the North American plate is concentrated mainly on the boundaries of three blocks, which are assumed to be relatively rigid. In the following discussion, the plate and block boundaries will be described first, then the motions within the model will be given, and finally the historic seismicity will be discussed and related to the model.

1. Plate and block boundaries

The tectonic setting and major boundaries are illustrated in Figure 1. The Yakutat block (YB), which has been described by Plafker and others (1978), is bounded by the Transition zone (TZ), the Fairweather fault (F), and the Pamplona zone (PZ) which passes through Icy Bay (I). Northwest of the Yakutat block is the Wrangell block (WB). The Wrangell block is bounded on the northeast by the Denali (D), Totschunda (T), and an inferred connecting fault between the Totschunda and Fairweather faults, and on the south by the Pamplona zone (PZ) and the Aleutian megathrust (AM). The northwestern boundary of the Wrangell block is speculative; it is tentatively assumed to diverge southward from the Denali fault, pass through Cook Inlet (CI), around Kodiak Island (KO) and back to the Aleutian megathrust. The St. Elias block (SE) is bounded by the Totschunda-Fairweather system on the southwest and by the Duke River (DR), Dalton (DA), and Chatham Strait (C) faults on the northeast.

The extent and configuration of the Pacific plate underlying Alaska can be inferred, at least partly, from the distribution of subcrustal earthquakes that make up the Benioff zone. These events occur within the underthrust oceanic plate near its upper surface. The 50-km isobath of earthquake foci shown in Figure 1 northwest of the Aleutian megathrust (AM) represents an active Benioff zone (Lahr, 1975).

The continuity of the Pacific plate below the Gulf of Alaska and the hundreds of kilometers of convergence indicated by the Benioff zone northwest of Prince William Sound imply that a similar amount of convergence has taken place in the zone between Prince William Sound and the Queen Charlotte Islands fault. The queried 50-km isobath in Figure 1 is the position for the underthrust Pacific plate suggested by Lahr and Plafker (1980) based on two assumptions: (1) the andesitic Wrangell

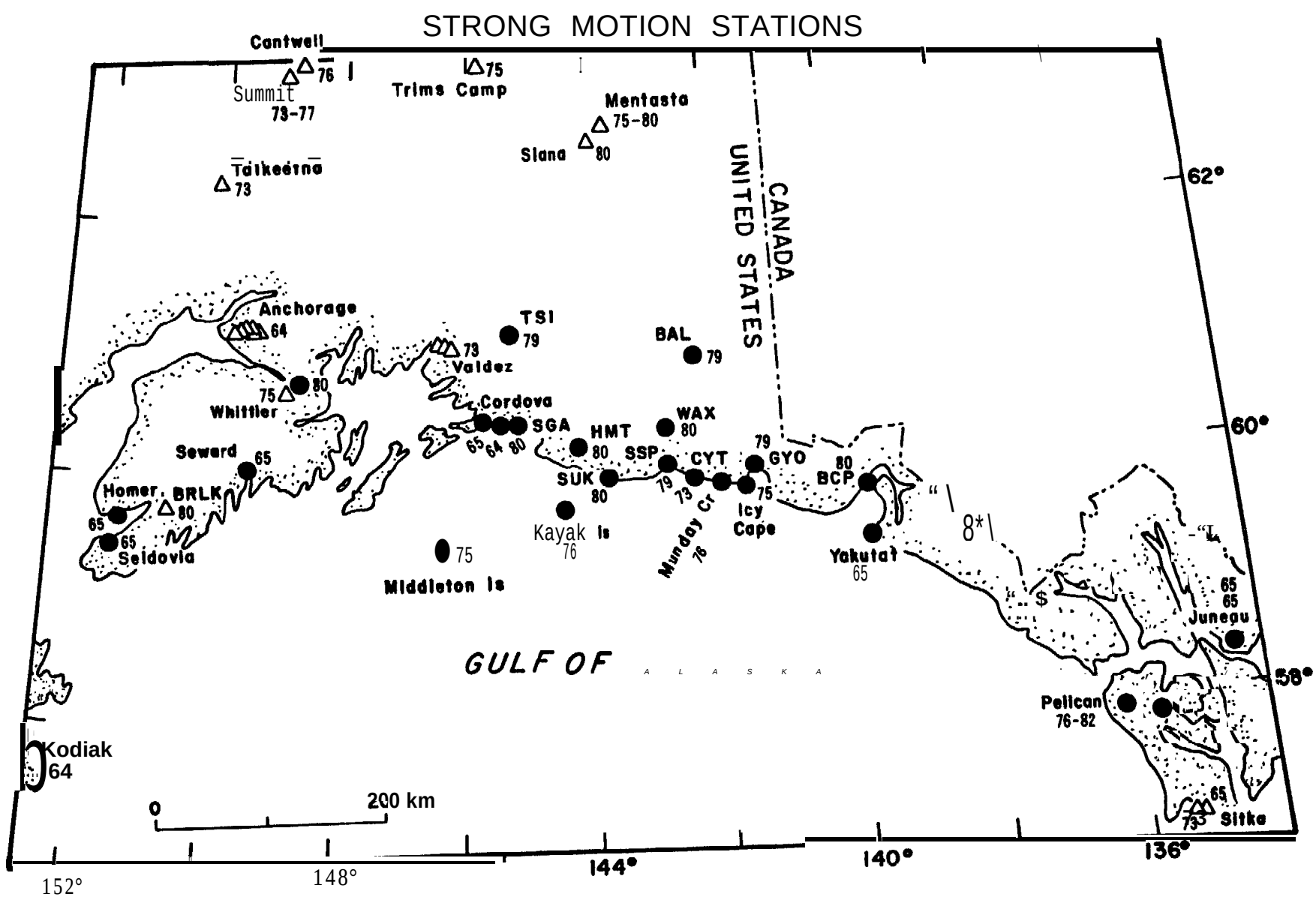

Figure 3. Location of USGS strong-motion instruments in southern Alaska showing year(s) of installation (and removal). Stations which were maintained at least in part with OCSEAP funds are indicated by solid circles. For Anchorage and Valdez, the year of the earliest installation is given.

volcanic rocks (Deninger, 1972; MacKevett, 1978) are situated above the 100-km isobath of the Benioff zone, as is typical for andesitic volcanoes associated with an underthrust plate, and (2) the dip of the plate between 50 and 100 km depth (about 40°) is similar to that observed elsewhere along the Aleutian arc (35° to 45*; Davies and House, 1979). Analysis of seismic data from the local seismic network has since confirmed the presence of a north-northeast dipping Benioff zone south of the Wrangells (Stephens and others, 1983) between 143° and 145° W longitude. Although the deepest event so far located has a depth of only 85 km, extrapolation of the zone to deeper depths would place Mounts Wrangell and Drum above events in the 100 to 125 km depth range. It therefore seems likely that the Pacific plate extends at shallow depths below much of the Yakutat and Wrangell blocks, a configuration that should be conducive to significant coupling between those blocks and the Pacific plate.

2. Plate motions in model

Motions in the kinematic model are relative to the stable parts of the North American plate, and in particular the interior of Alaska. This kinematic model was developed to be as compatible as possible with historical seismicity and known rates of relative plate movement (Lahr and Plafker, 1980).

The Pacific plate rotates relative to North America about a pole in eastern Canada and moves northwestward at 5.8 cm/yr along the Queen Charlotte Islands fault (Figure 4). The relative velocity increases to the southwest as distance from the pole of rotation increases. The Yakutat block moves parallel to the Pacific plate but with a slightly lower relative velocity (5.4 cm/yr). Motion of the Wrangell block is counterclockwise rotation about an axis near Kodiak Island, such that its northeastern edge moves in a right-lateral sense relative to the North American plate with a velocity of approximately 1 cm/yr. The St. Elias block moves roughly parallel to the Pacific plate with a relative velocity of 0.2 cm/yr. A cross section through the model is given in Figure 5.

3. Historical seismic record

The instrumental seismic history of the eastern Gulf of Alaska region, prior to the installation of a local network in 1974, is limited in terms of both completeness and accuracy by the lack of nearby seismograph stations. The record for events larger than 7-3/4 is probably complete only since 1899; for events larger than 6 since the early 1930's; and for events larger than 5 since the 1964 Alaska earthquake (Page, 1975; Homer, in press).

Figure 6 shows the distribution of earthquakes from 1900 through March 28, 1964, the date of the 1964 Alaska earthquake. Most of these data are from the Earthquake Data File (EDF) of NOAA. The magnitude used for scaling in the figures is the maximum of the m_b, Mother (usually BRK or PAS magnitude), and M_L (PMR, the NOAA Alaska Tsunami

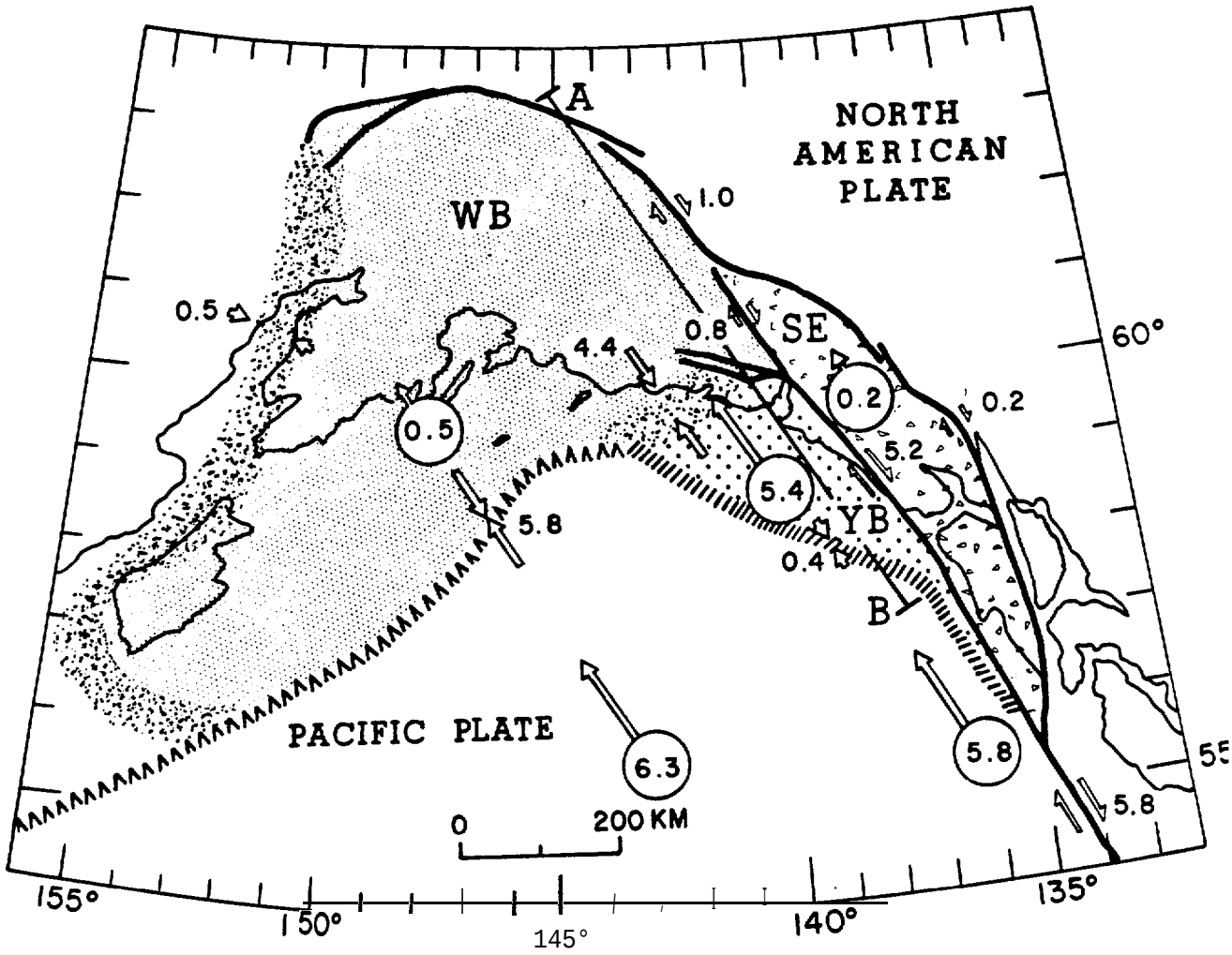

Figure 4. Proposed model for present crustal deformation along Pacific-North American plate boundary in southern and southeastern Alaska. Circled numbers give rate of motion (centimeters per year) of Pacific plate, Yakutat block (YB), St. Elias block (SE), and Wrangell block (WB) relative to North American plate. Numbers next to paired vectors give rate of motion across indicated zone. Stippled bands mark surface outcrops of major zones of deformation and faulting. A-B, location of cross section shown in Figure 5.

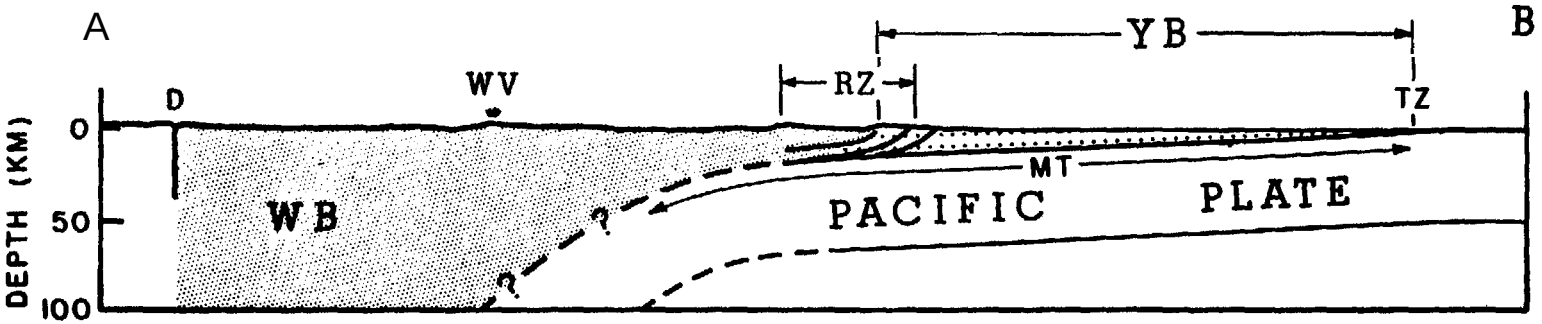

Figure 5. Diagrammatic structure along plane A-B of Figure 4. Abbreviations are: **MT** - main thrust; **WB** - **Wrangell** block; **YB** - **Yakutat block; WV** - **Wrangell volcanics;** D - **Denali** fault; RZ - rupture zone of February 28, 1979, earthquake; **TZ** - transition zone. **No** vertical **exaggeration.**

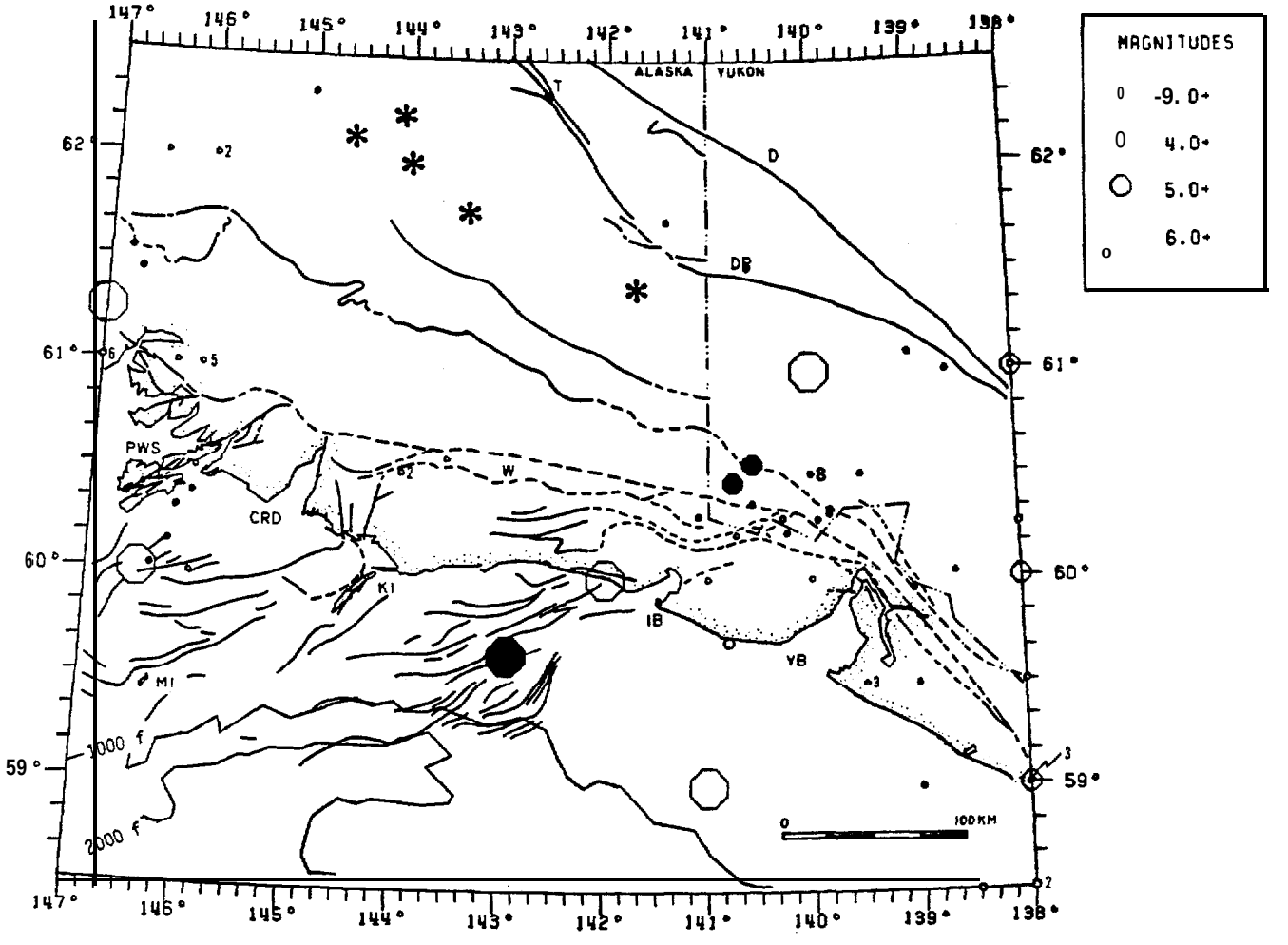

Figure 6a. Map of epicenters for 80 historic earthquakes that occurred between January 1, 1900 and March 28, 1964. Numbers next to epicenters indicate total number of events in cases where more than one event occurs at the same location with the same magnitude. Filled symbols mark the more accurate epicenters, and are repeated in Figure 7. Symbol size is proportional to magnitude as indicated at the upper right. Faults after **Beikman** (1980), Bruns (1979), and **Clague** (1979). Volcanic cones (stars) after King (1969). Abbreviations are: **CRD** - Copper River Delta; D **Denali** fault; DR - Duke River fault; **IB** - Icy Bay; **KI** - Kayak Island; MI Middleton Island; **PWS** - Prince William Sound; W - Waxen Ridge; and **YB** **Yakutat** Bay. All but one of the events indicated to be less than magnitude 4.0 have no magnitude reported, so many of these events are likely to be larger than indicated.

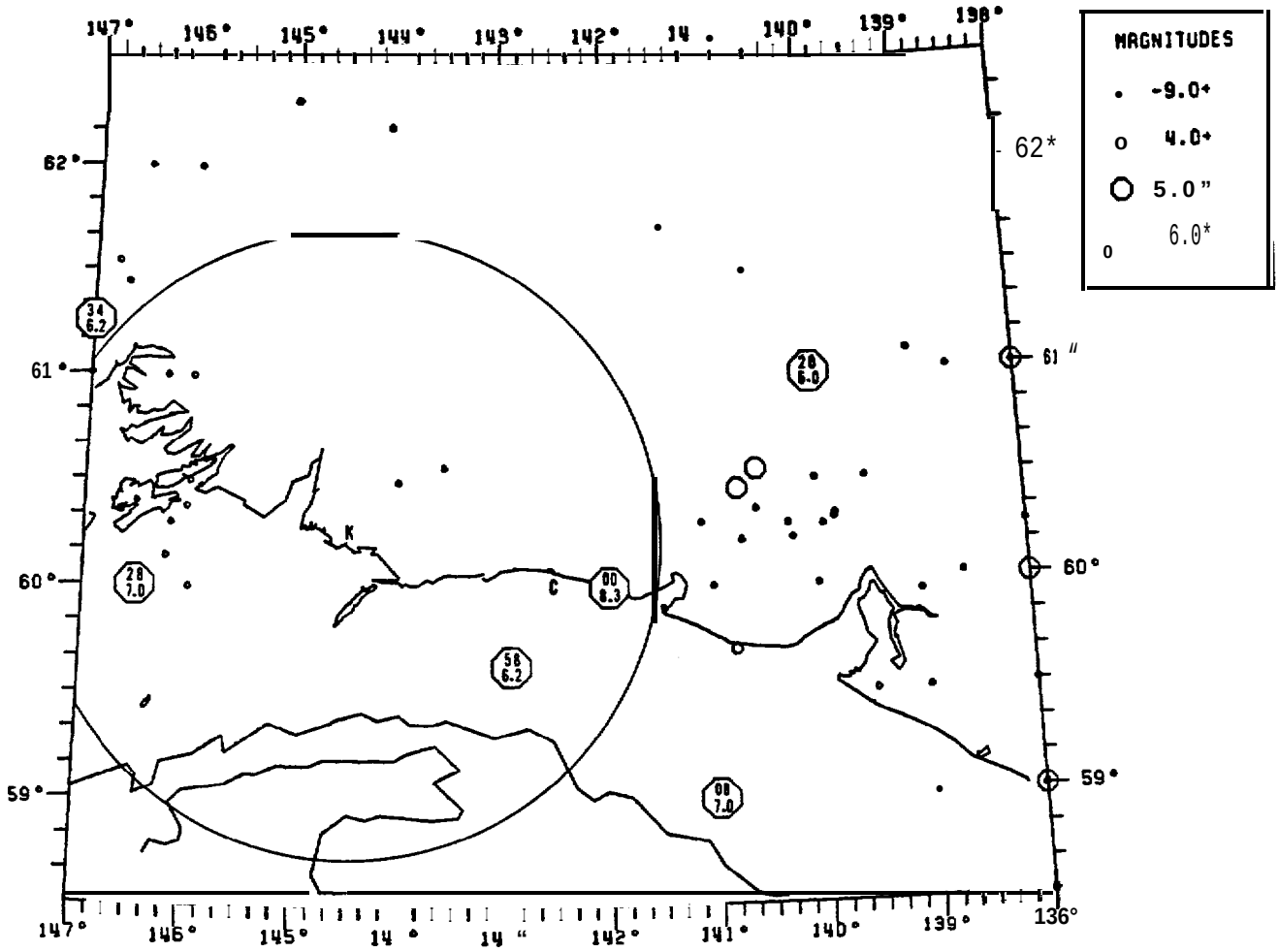

Figure 6b. Historic epicenters, as in Figure 6a, except year and magnitude are indicated for events greater than or equal to 6.0. Abbreviations are: **K - Katalla;** and C - Cape **Yakataga.** Circle encloses **epicentral** location of 1908 event, as inferred from the intensity at **Katalla.**

Warning Center, formerly Palmer Observatory) magnitude as given in the EDF file. Epicenters for 24 of the events that occurred between 1954 and 1959 are from published relocations (Tobin and Sykes, 1966; Tobin and Sykes, 1968; Sykes, 1971). The 24 relocated events are shown again in Figure 7 along with the location given in the EDF. Tobin and Sykes (1966) estimate that many of the relocated events have epicentral standard errors less than 10 to 20 km as compared to errors as large as 100 km that were common previously. They note, however, that the accuracy of the epicenters could be less than that suggested by the standard errors if there is a regional bias in the locations. Figure 7 gives a graphic indication of the uncertainties in the historic locations.

The large event shown just west of Icy Bay occurred on October 9, 1900, with a magnitude of 8.1 (Richter, 1958; Thatcher and Plafker, 1977). Based on macroseismic effects McCann and others (1980) conclude that this event actually occurred in the vicinity of Kodiak Island, several hundred kilometers southwest of Icy Bay. However, two great (M_S|8) earthquakes that occurred in 1899 produced uplift of as much as 14 m near Yakutat Bay (Tarr and Martin, 1912), and may have ruptured across much of the coast between Yakutat Bay and Kayak Island (McCann and others, 1980). These events occurred within the complex northern corner of the Yakutat block and possibly along the Pamplona zone of thrusting.

The magnitude 7.0 earthquake of 1908 southeast of Icy Bay was located to the nearest degree by Gutenberg and Richter(1954) using arrival times from 11 stations including Sitka (based on Gutenberg and Richter's notes provided by W.H.K. Lee, U.S.G.S.). Gutenberg and Richter's notes include "near Yakataga IX-X"', probably reflecting the intensity at Cape Yakataga (C in Figure 6b). The Earthquake History of the United States (1973) includes "At Katalla, there were sharp shocks in rapid succession during which buildings rocked. Rockslides were reported at Yakataga. Felt from Sitka to Seward.*' The rockslides at Katalla (K in Figure 6b), which may account for the assignment of intensity IX to X, are now thought to be a poor determinant of intensity (Stover and others, 1980). Tarr and Martin (1912) report that the shock was felt slightly at Sitka but generally at Seward. The Katalla Herald newspaper article of May 16, 1908 (Tarr and Martin, 1912) states that the earthquake "'set every building in town rocking, moved furniture about rooms, knocked dishes from shelves, and caused many of the people in town, many of whom had retired, to take to the streets."' Based on this description, the Modified Mercalli intensity was about VI at Katalla. The 1979 St. Elias earthquake occurred 165 km from Katalla and had a comparable magnitude to the 1908 event. The intensity map of Stover and others (1980) implies that the intensity at Katalla due to the 1979 event was within the V - VI range. Therefore the location of the 1908 earthquake was probably within 165 km of Katalla (see Figure 6b). Due to the location uncertainty it is not possible to determine which fault zone ruptured during the 1908 event.

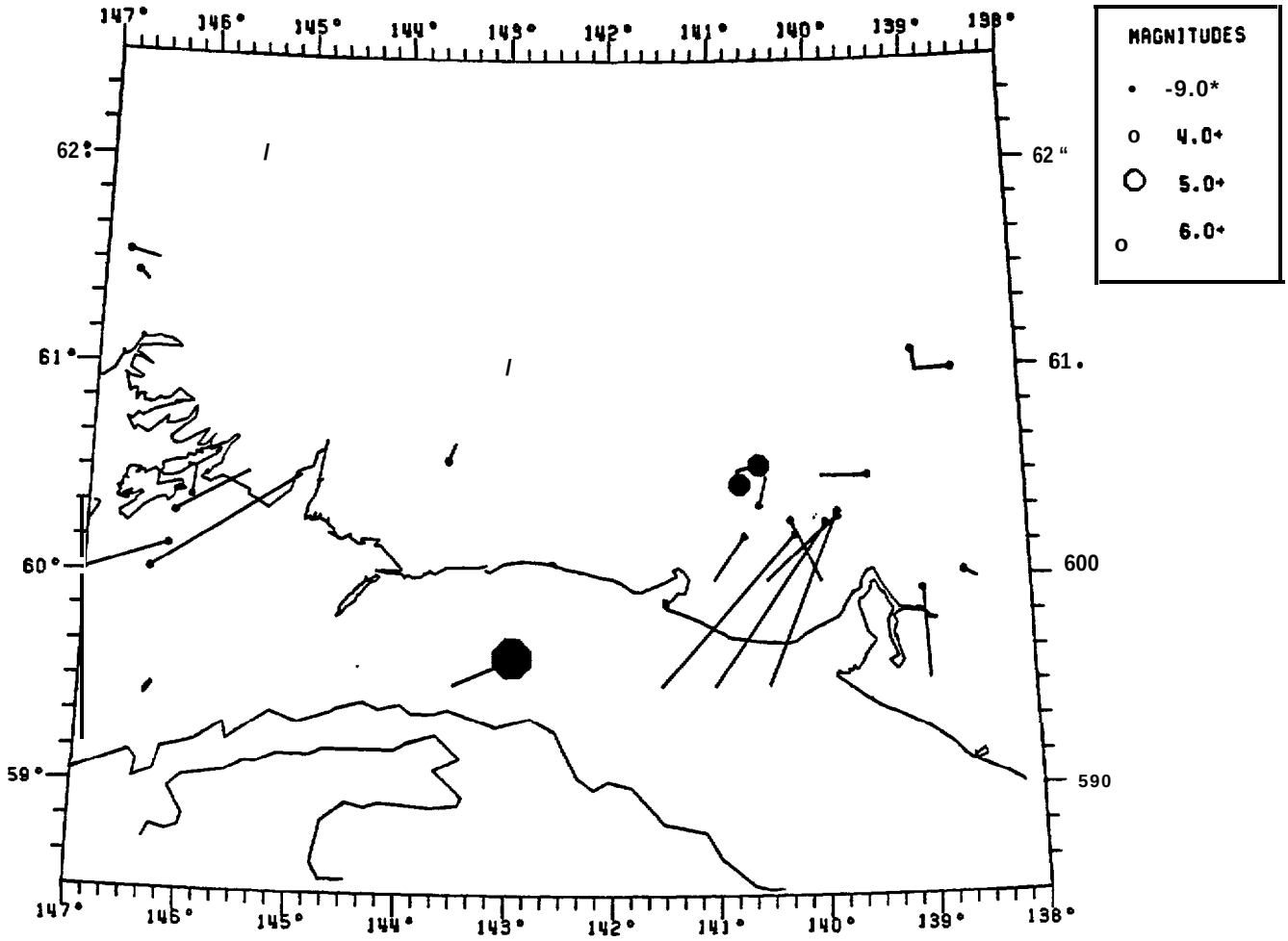

Figure 7. Epicenters of 24 relocated earthquakes (Tobin and Sykes, 1966; Tobin and Sykes, 1968; Sykes, 1971) that occurred between 1954 and 1959 (solid symbols) with a line extending to the location given in the Earthquake Data File.

In 1928 a magnitude 7.0 earthquake occurred south of Prince William Sound, probably on the shallow dipping Aleutian megathrust interface. During the 1964 earthquake secondary faulting occurred within the Wrangell block on the Patton Bay and Montague Island faults. We cannot preclude the possibility that the 1928 event could have been of the latter type. A third possibility, although less likely for an earthquake of this size, is that it occurred within the Pacific plate that is underthrusting the Wrangell block.

Epicenters of events that occurred within 2 weeks of the 1958 earthquake on the Fairweather fault (Ms 7.9; Tobin and Sykes, 1968; Sykes, 1971) are shown in Figure 8. The rupture zone extended from north of Yakutat Bay to Cross Sound, a total distance of about 325 km (Tobin and Sykes, 1968). Fault slip was predominantly right-lateral strike-slip, with the largest offset measuring 6.5 m (Tocher, 1960). The rate of relative motion across the Fairweather fault (which bounds the Yakutat and St. Elias blocks) has probably averaged at least 4.8 and more probably 5.8 cm/yr in a right-lateral sense for at least the past 1,000 years (Plafker and others, 1978). This rate is in reasonable agreement with the model rate of 5.2 cm/yr (Figure 4).

The 1964 Alaska earthquake was one of the largest earthquakes in history, being produced by an average of 12 meters of dip slip motion on a fault plane approximately 200 km wide, 600 km long, and dipping 4° to the northwest (Hastie and Savage, 1970; Page, 1968; Plafker, 1969). Earthquakes that occurred during the first two weeks following the Alaska earthquake are shown in Figure 9.

The severe damage to the coast of south-central Alaska produced by vertical displacements, subaqueous slides, and destructive tsunamis is described by Plafker and Mayo (1965) and is repeated here to illustrate the possible effects of a great earthquake within the eastern Gulf of Alaska region.

> "Notable changes in land level occurred over an area in excess of 50,000 square miles [130,000 square kilometers] in a broad northeast-trending belt more than 500 miles [800 kilometers] long and as much as 250 miles [400 kilometers] wide, which lies between the Aleutian Trench and the Aleutian volcanic Arc. The northwest part of this belt, which includes most of the Kenai Peninsula and the Kodiak Island group, sank as much as 7.5 feet [2.3 meters], bringing some roads, rail lines, docks, and settlements within reach of high tides and producing a fringe of salt-water-killed vegetation along the drowned coasts. The area to the southeast, including most of Prince William Sound and the adjacent continental shelf as far south as southern Kodiak Island, rose generally 4 to 8 feet [1.2 to 2.4 meters], and locally at least 33 feet [10.1 meters]. Some beaches and surfcut platforms were permanently raised above the reach of tides, resulting in mass extermination of intertidal faunas and floras and impaired usefulness of harbors, channels, and many shoreline installations."'

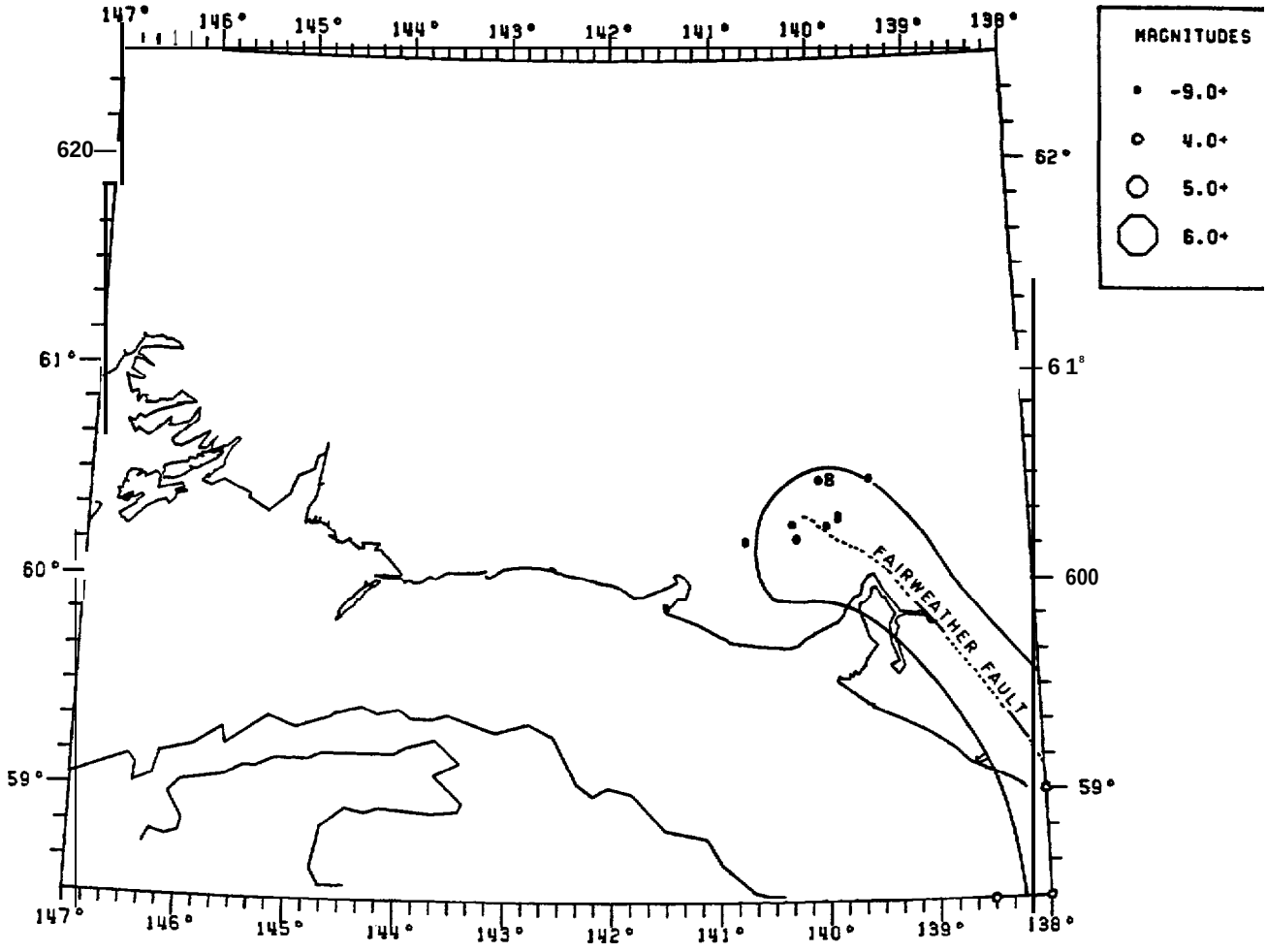

Figure 8. Epicenter map of the 19 events that occurred within two weeks of the July 10, 1958 earthquake on the Fairweather fault. 1958 rupture zone after McCann and others (1980). Filled symbols are relocated events from **Tobin** and Sykes (1966, 1968) and Sykes (1971).

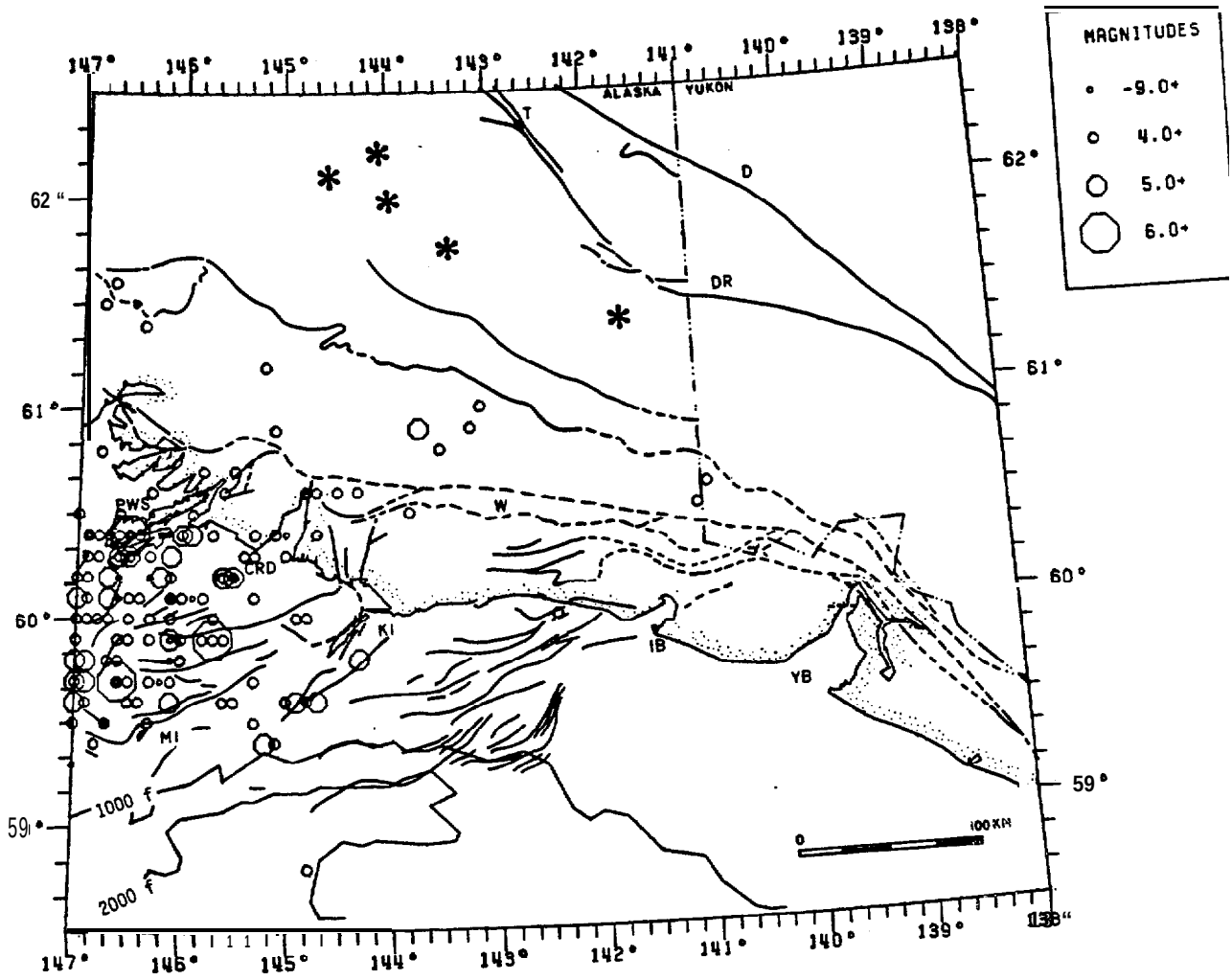

Figure 9a. Map of epicenters for 155 earthquakes that occurred between March 28, 1964 and **April** 12, 1964, the first two weeks following the 1964 Alasks earthquake. Symbols and labels same as Figure 6a.

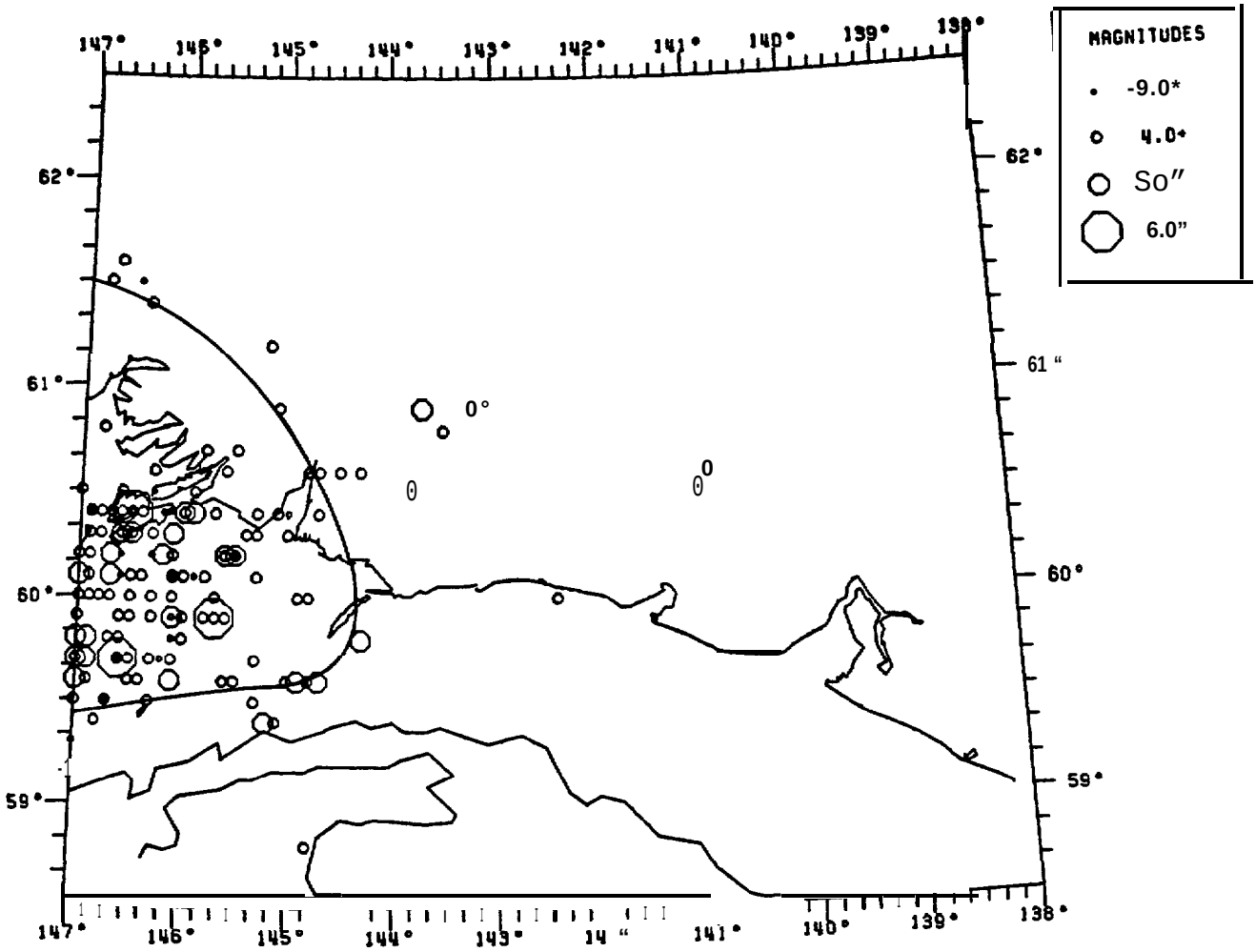

Figure 9b. Epicenters during first two weeks following the 1964 earthquake, as In Figure 9a. The eastern boundary of tne 1964 rupture zone, as defined by McCann and others (1979), is shown.

*'Surface faulting was confined to Montague Island, and was dominantly vertical and subsidiary to regional uplift. Of the two known faults one has been traced more than 16 miles [26 kilometers] on land and about 15 miles [24 kilometers] in the submarine topography to the southwest of the island. Maximum measured vertical fault displacement on land was 16 feet [4.9 meters] on one fault and about 18 feet [5.5 meters] on the other."

"Submarine uplift of the continental shelf generated a train of long-period large-amplitude seismic sea waves, the first of which struck the outer coasts of the Kenai Peninsula and Kodiak Island between 19 and 30 minutes after the initial shock. The highest waves inundated shorelines locally to elevations of 35 to 40 feet [10.7 to 12.2 meters], causing 20 deaths and damage to property all along the coast of the Gulf of Alaska, especially in those areas that had been lowered relative to sea level by tectonic subsidence. The sea waves were recorded on tide gauges throughout the Pacific Ocean and resulted In casualties and local damage at points as distant as British Columbia, Oregon, and California."

"The earthquake caused widespread subaqueous sliding and sedimentation in Prince William Sound, along the south coast of the Kenai Peninsula, and in Kenai Lake. These slides carried away the port facilities of Seward and Valdez and the small boat harbor at Homer. Local violent surges of water, many of which were generated by known subaqueous slides that occurred during the earthquake, left swash marks as much as 170 feet [51.8 meters] above water level and caused heavy damage and took 85 lives at Seward, Valdez, Whittier, Chenega, and several smaller communities in Prince William Sound.*'

The seismicity during the ten years following the 1964 Alaska earthquake is shown in Figure 10. Epicenters are from bulletins of the International Seismological Center (ISC) and magnitudes are the maxima of the ISC m_b, EDF mb, EDF Mother (usually Ms at BRK or PAS), and the EDF ML (Palmer). Activity is dominated by events within and adjacent to the 1964 rupture zone. Offshore activity is approximately bounded on the south and east by the 1000 fathom isobath and the Pamplona zone. Two notable concentrations occur along this boundary, one near 145° W and the other along the Pamplona zone. The rate of activity near 145°W was highest just following the 1964 earthquake. The rate decreased steadily to a low level by the end of 1965 and remained low except for a sequence in mid-1969 that included three magnitude m_b 5 events. The Pamplona zone activity of Figure 10 occurred during two swarms. The first consisted of ten events ranging up to magnitude m_b 5.3 during April and May 1964, while the second consisted of 13 events during April 1970, the largest event having magnitude M_S 6.8. The temporal clustering of the Pamplona zone shocks contrasts with the more nearly continuous activity within the cluster northeast of Icy Bay.

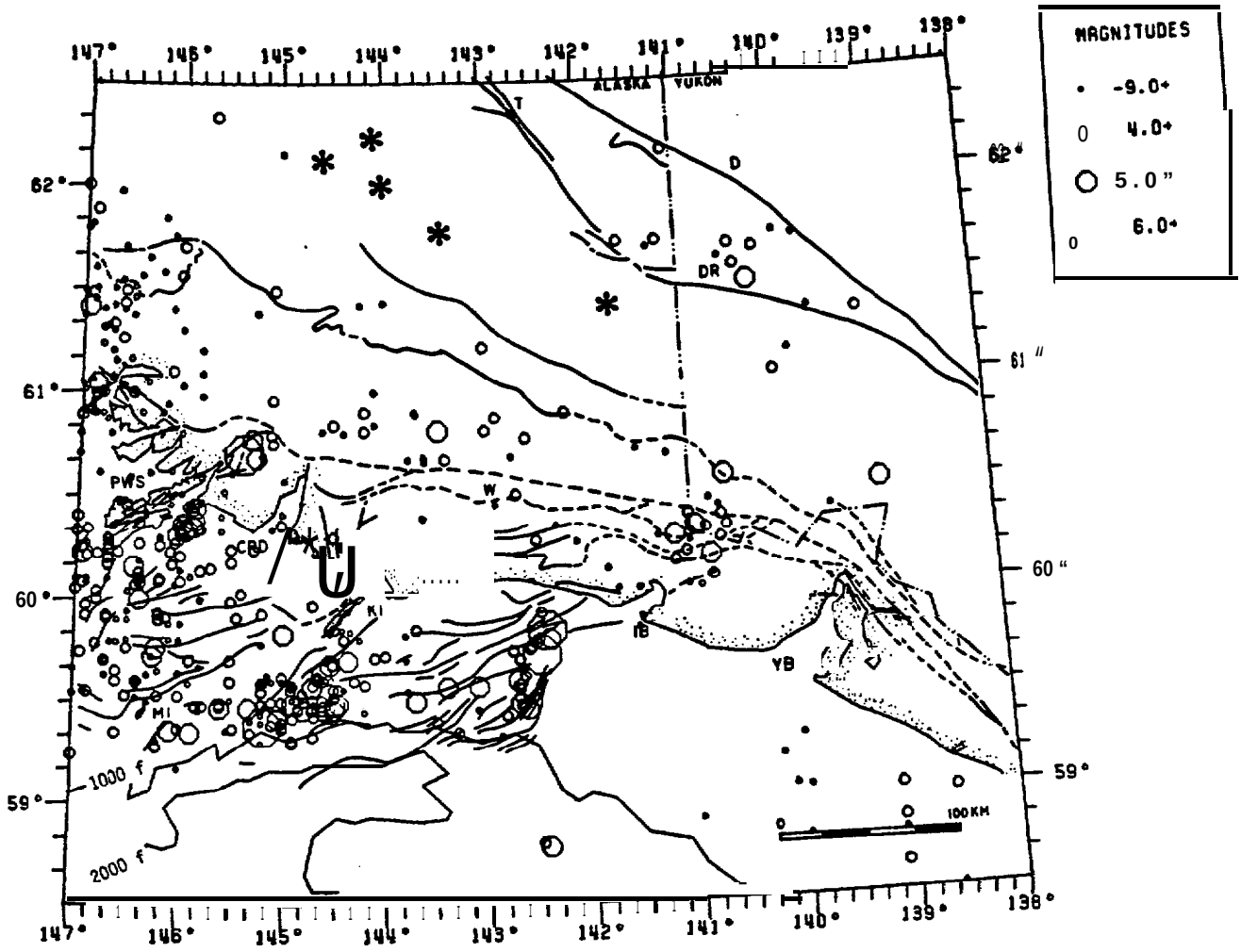

Figure 10a. Epicenter map of 453 earthquakes that occurred between April 13, 1964 and September 30, 1974. Symbols and labels same as Figure 6a.

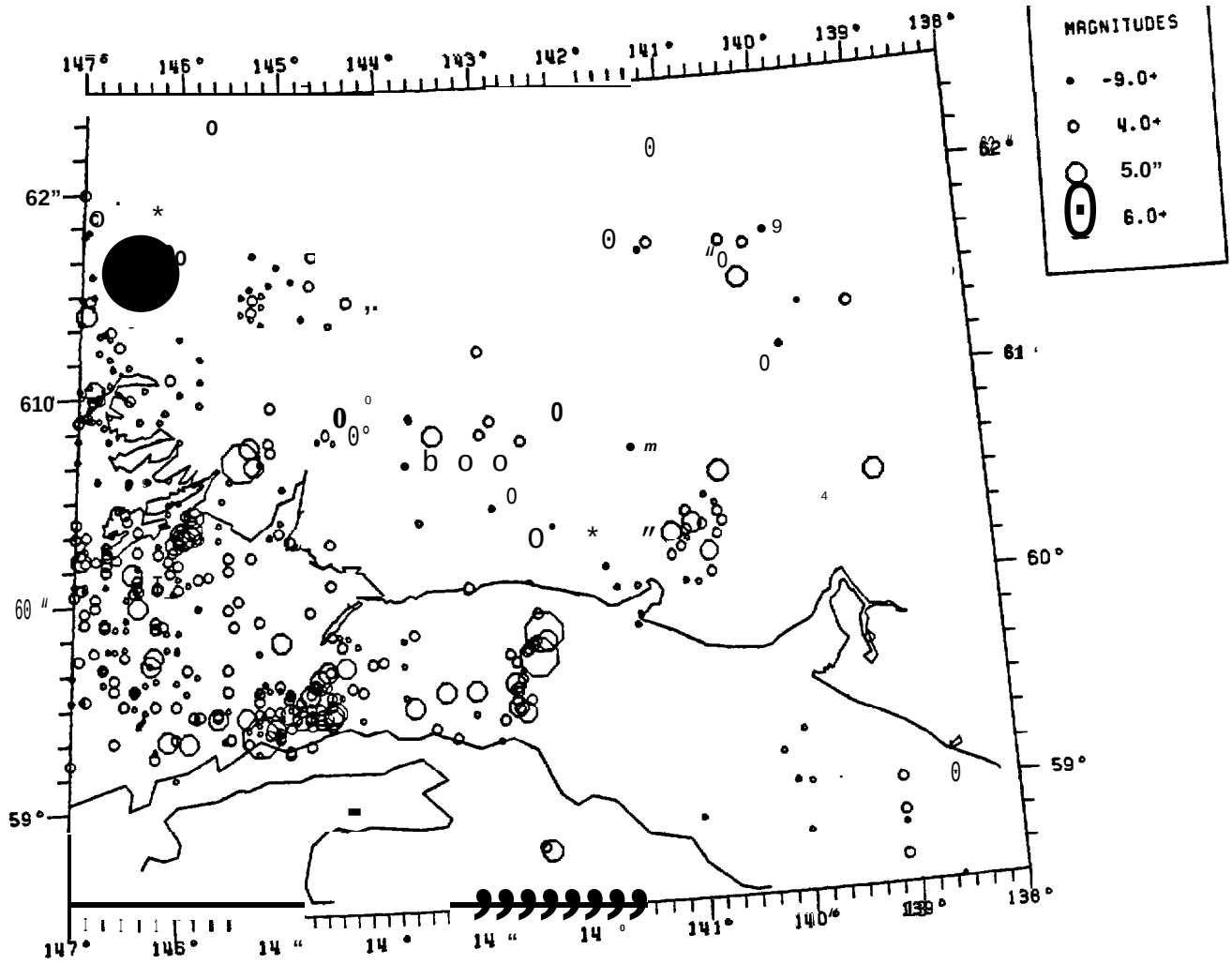

Figure 10b. April 13, 1964 through September 30, 1974 epicenters, as in Figure 10a.

Focal mechanisms were determined for two of these events by Perez and Jacob (1980), and both were consistent with underthrusting on a shallow dipping plane, one in a north-northeast direction and the the other in a north-northwest direction. These mechanisms are in general agreement with the proposed model, except that northwest-southeast oriented convergence would be expected between the Yakutat and Wrangell blocks.

B. Seismicity during 1974 - 1981

In September 1974 the seismographic coverage of the eastern Gulf of Alaska was greatly enhanced by the installation of thirteen new stations between Montague Island and Yakutat Bay. This coverage made it possible to routinely monitor seismic activity as small as magnitude 1.0 and to locate events with increased accuracy. Except for gaps that total 1.75 years due to instrumental and operational difficulties, preliminary processing is complete for October 1974 through September 1981. For this period a total of 9647 hypocenters has been determined, which is 14 times greater than the total number located prior to October 1974.

The magnitudes calculated from the local network data are systematically offset to smaller values as compared to the EDF magnitudes. For example, Figure 11 shows the EDF m_b magnitude plotted versus the coda magnitude for events in the region 138° - 147*W, 58.5° - 62.5° N for October 1974 through November 1980. In order to present a complete picture of the most significant earthquakes since 1974, all events with EDF magnitude greater than or equal to 4 were processed using the local network to determine both location and magnitude. Based on the distribution of Figure 11, this sample should contain all events of coda magnitude 3.5 or larger.

In Figure 12, the distribution of events of coda magnitude 3.5 and greater that occurred between October 1, 1974 and September 31, 1981 is shown. Note that, relative to earlier figures, there is a shift of 0.8 magnitude units in the limits chosen for symbol size. This technique was employed so that the earthquakes on this plot would not appear smaller than earthquakes of comparable magnitude in the previous figures. The largest event is the 1979 St. Elias earthquake north of Icy Bay which had a magnitude M_s 7.1 (Buland and Taggart, 1981), and most of the events north and east of Icy Bay in Figure 12 are St. Elias aftershocks. The two next largest events lie offshore near the 1,000 fathom isobath and near the southern limit of seismicity noted in Figure 10.

The seismic data obtained during 1974 - 1981 (Figures 13-17) have provided important constraints for the development of a regional tectonic model. One of the key results from this monitoring is the detailed recording of the aftershock sequence of the large 1979 St. Elias earthquake (Stephens and others, 1980). The depth control provided by the local seismic stations helped to confirm that the rupture from this event was confined to a buried fault or fault system at shallow depth. Focal mechanisms determined from P-wave first-motions for the mainshock and several aftershocks are compatible with a teleseismically determined focal mechanism for the mainshock of low-angle thrusting on a northward-dipping

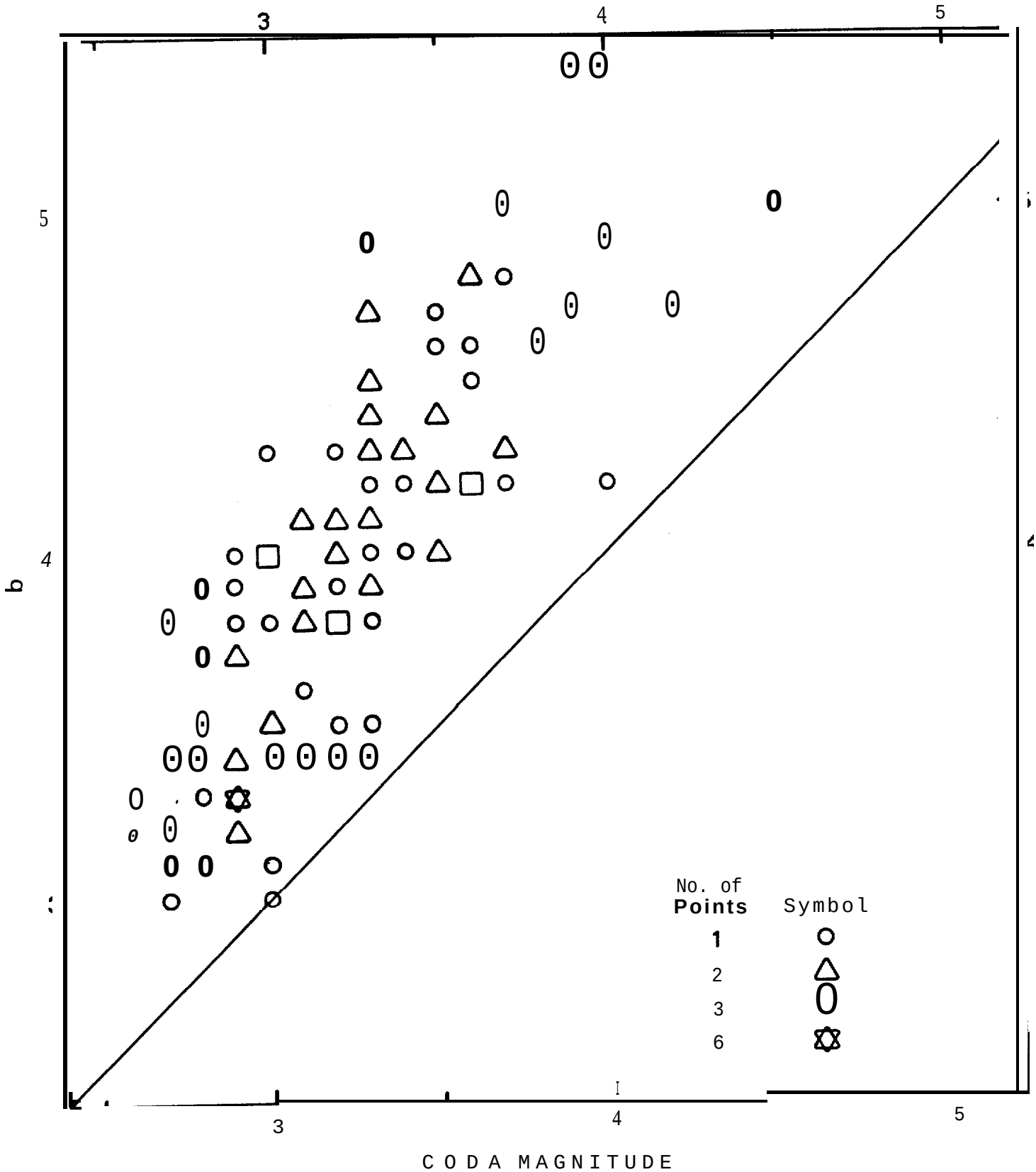

Figure 11. Plot of EDF body-wave magnitude (m_b) Versus coda magnitude calculated from local stations.

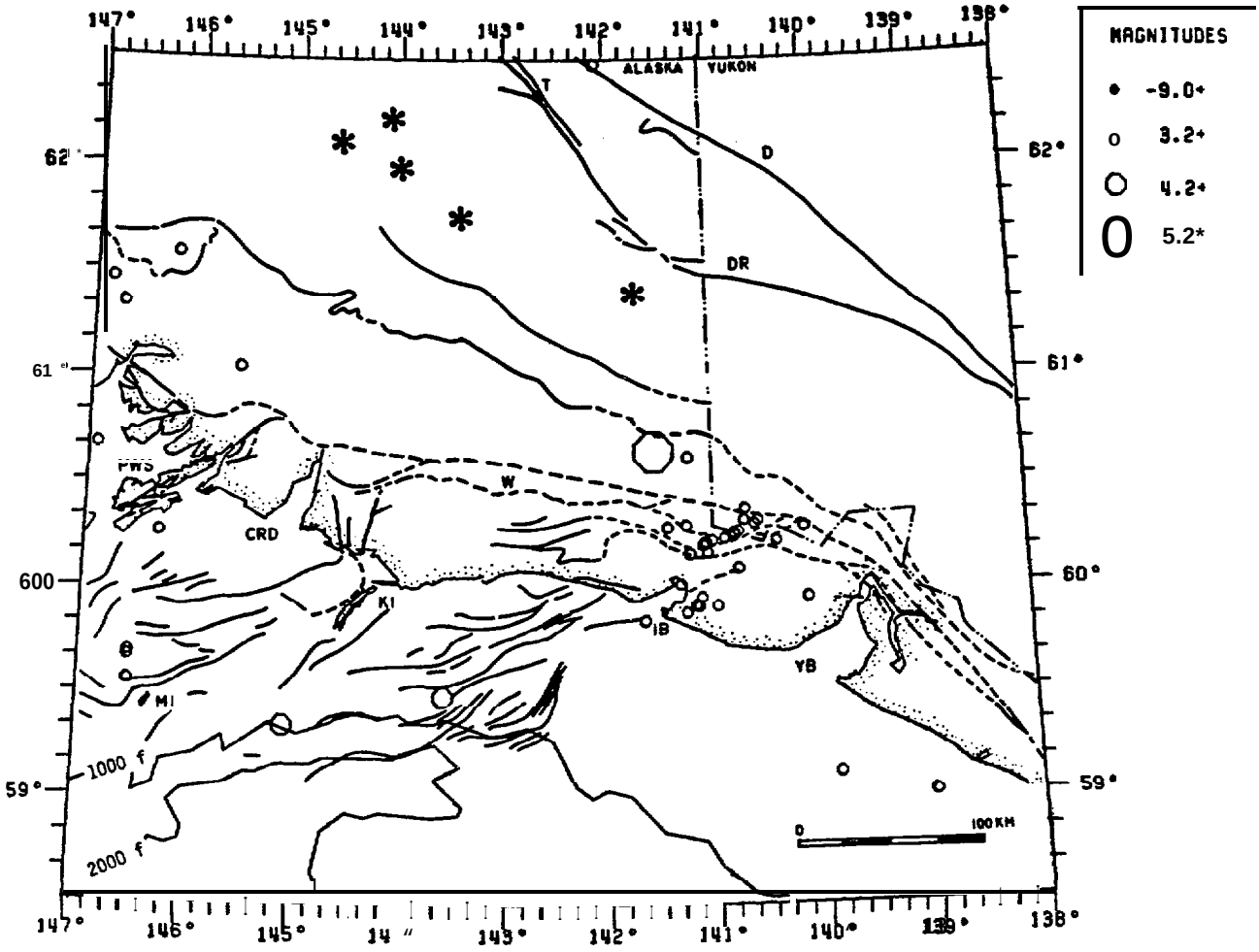

Figure 12a. Epicenter map of 42 earthquakes with coda magnitudes greater than or equal to 3.5 that occurred between October 1, 1974 and September 31, 1981. Labels same as Figure 6a. Note change in symbol sizes from previous figures.

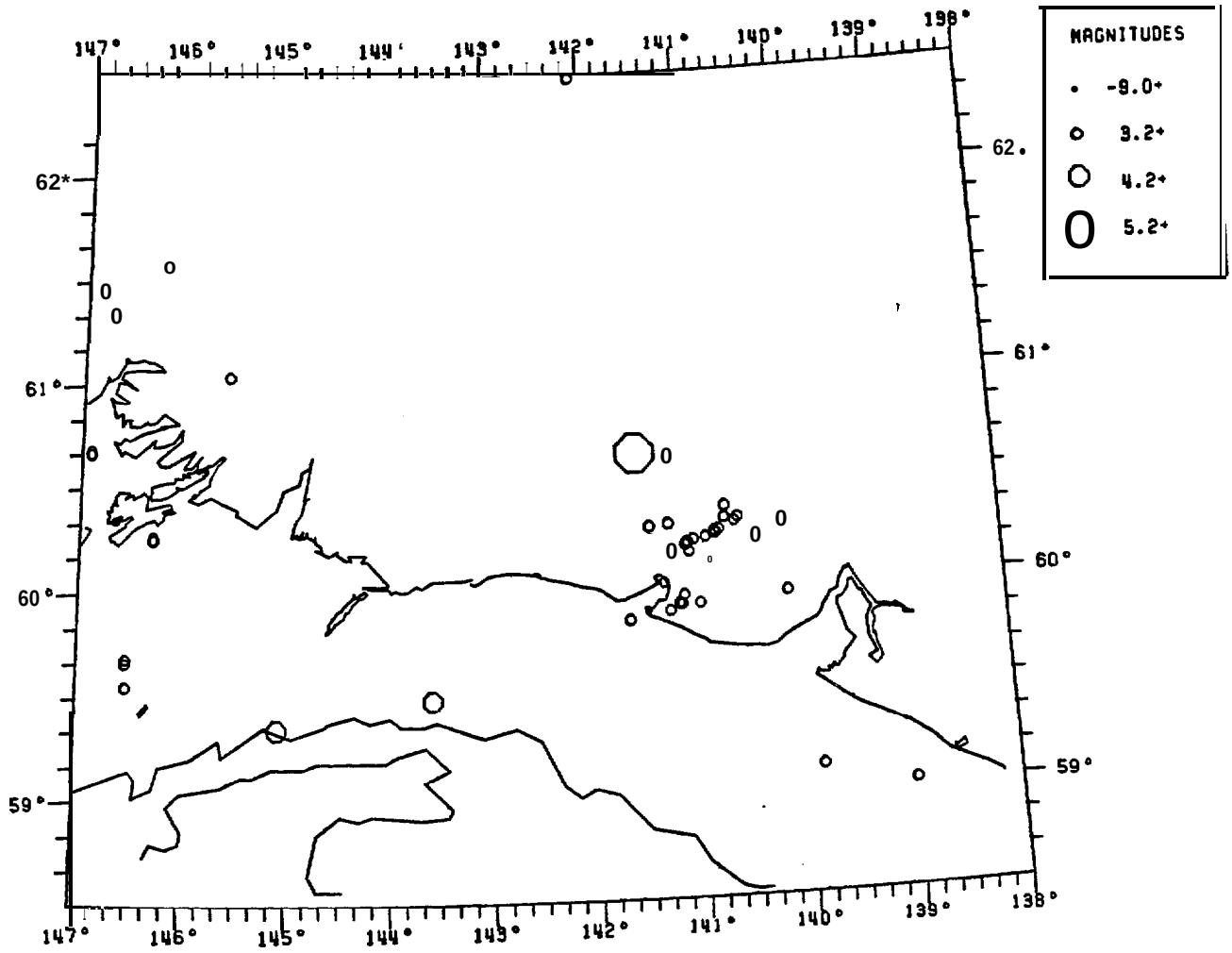

Figure 12b. October 1, 1974 through September 30, 1981 epicenters, as in Figure 12a.

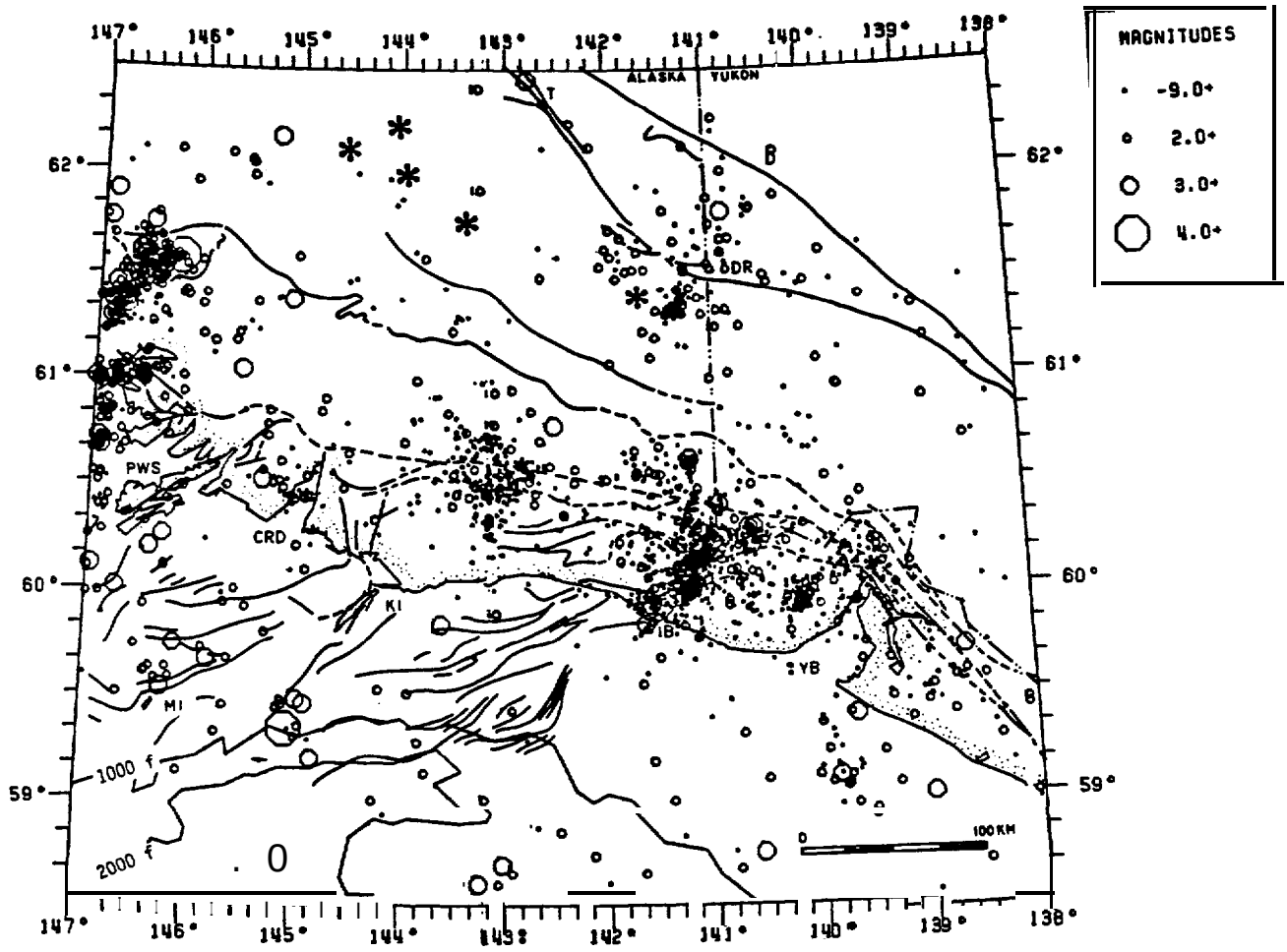

Figure 13a. Epicenter map of 2015 earthquakes located by the local seismograph network between October 1, 1974 and February 28, 1979 just prior to the **St. Elias** earthquake. Labels same as Figure 6a. Note that symbol sizes are larger than **in previous** figures.

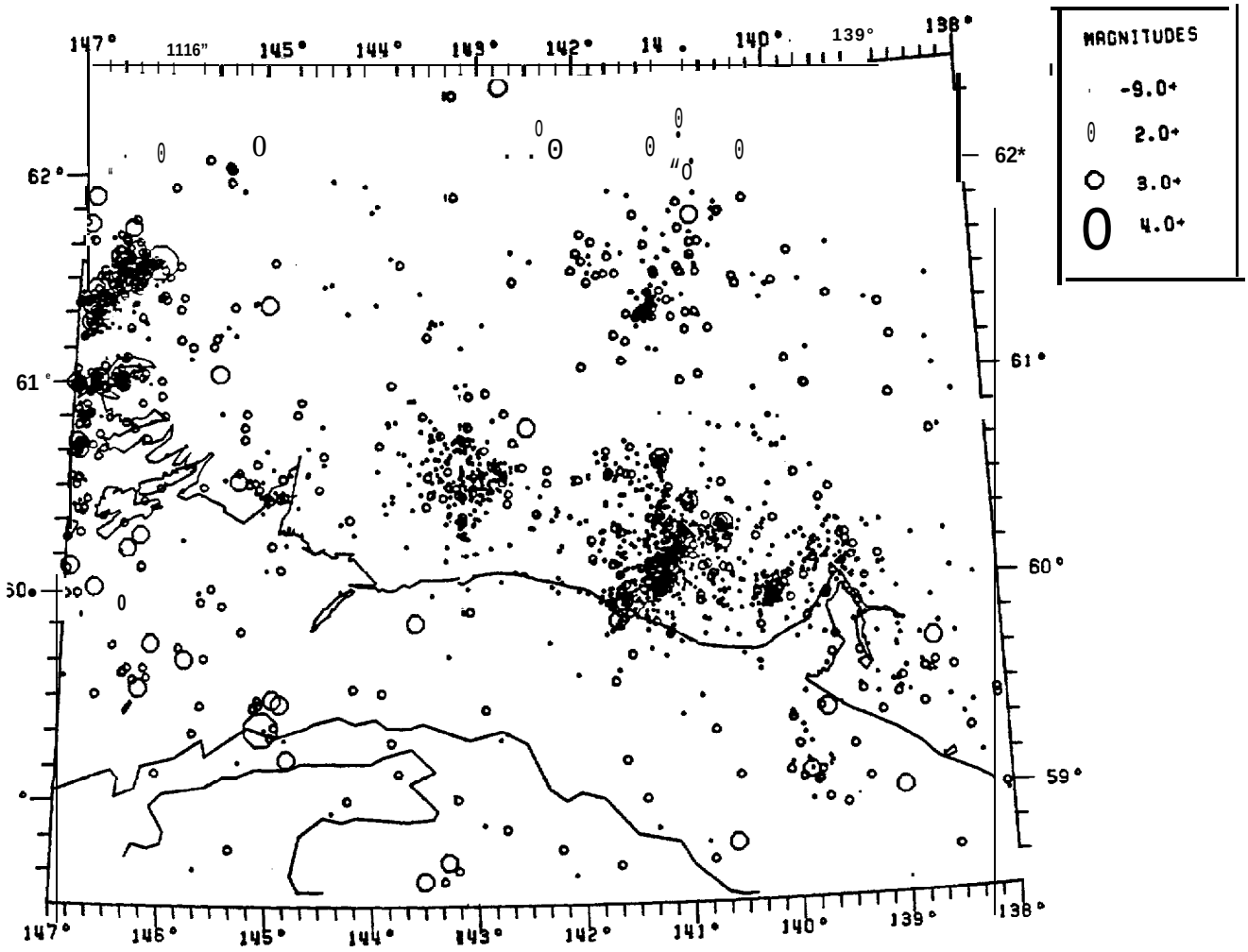

Figure 13b. October 1, 1974 through February 28, 1979 epicenters as in Figure 13a.

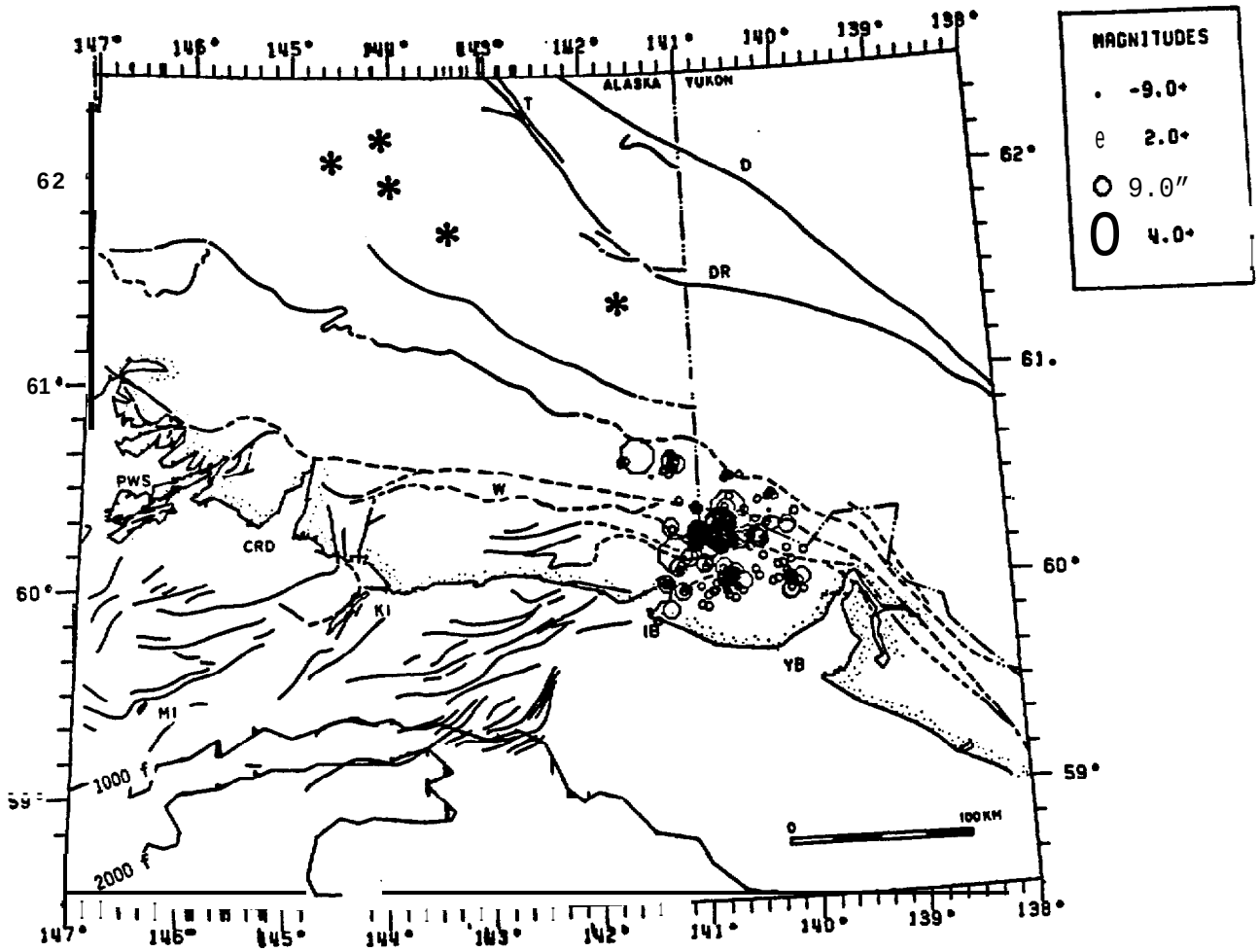

Figure 14a. Epicenter map of 287 earthquakes located by the local seismograph network starting with the St. Elias earthquake on February 28, 1979 through March 30, 1979. Labels same as Figure 6a.

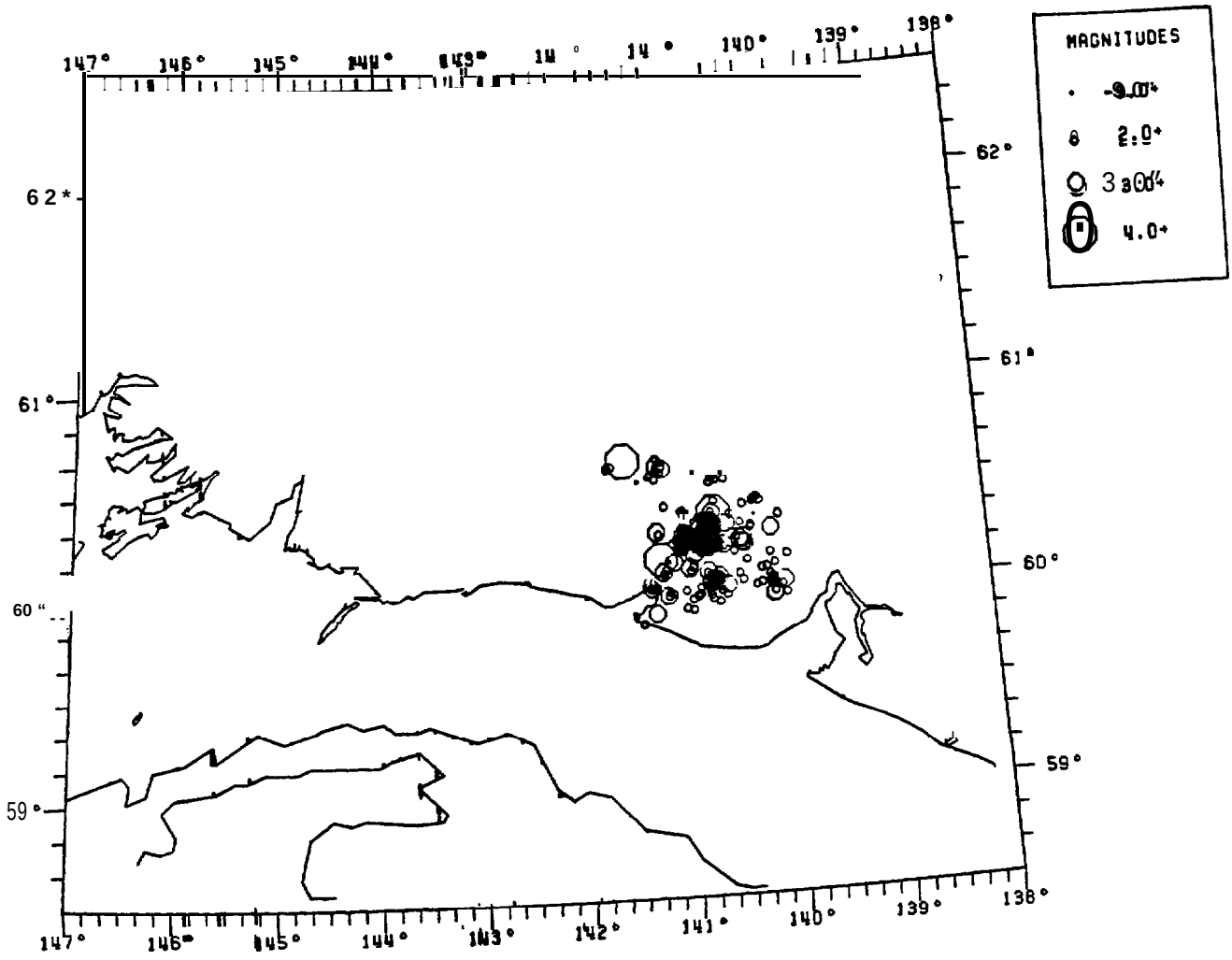

Figure 14b. February 28, 1979 through March 30, 1979 epicenters, as in Figure 14a.

plane. The distribution and dep-ths of the microearthquake activity west of the St. Elias aftershock zone suggest that the same buried fault system that ruptured during the St. Elias earthquake may extend at least 150 km farther to the west.

Another important result is the discovery of a north-northeast-dipping Benioff zone extending to a depth of 85 km south of the Wrangell volcanoes (Stephens and others, 1983). The geometry and orientation of this zone is compatible with the interpretation that the seismicity deeper than about 30 km occurs in the subducted Pacific plate. If this interpretation is correct, then it constrains the northern limit of the Yakataga seismic gap to be south of the 40 km isobath of the Wrangell Benioff zone (Davies and House, 1979). The approximate extent of the Yakataga seismic gap as defined by the rupture zones of the 1964 Alaska earthquake, the 1979 St. Elias earthquake, and the 40 km isobath is shown in Figure 18.

Other areas where notable concentrations of shallow seismicity have been identified include the Copper River Delta, the Waxen Ridge area 100 km northeast of Kayak Island, the Wrangell volcanic massif, and the Denali-Totschunda-Duke River fault system. Relocated hypocenters for the activity beneath the Copper River Delta concentrate in the depth range 20-25 km; many of the events are tightly clustered along a west-northwest-east-southeast trend that is oblique to mapped fault traces at the surface. This activity may be occurring within the subducted Pacific plate. Around Yakutat Bay the pattern of seismicity is more diffuse and may reflect distributed activity on the complex system of mapped strike-slip and inferred thrust faults. Within the seismicity distributed throughout the Wrangell Mountains are distinct sequences of events that are tightly clustered in space and time (see, for example, Stephens and others, 1982). One of these clusters is located near 62° N, 144° W (Figure 16) on the south flank of Mt. Wrangell and may be volcano-related, but in general the clusters have not occurred near the principal volcanoes. Near the strike-slip Denali fault and the Duke River thrust fault system the seismicity is aligned along trends offset to the south from but approximately parallel to the faults. This offset is thought to be the result of systematic errors in locations due to incorrect velocity modeling and large gaps in station coverage, which is confirmed by Homer (1983) who finds little or no offset for earthquakes that have control from nearby Canadian stations. These sections of the Denali and Duke River faults are therefore thought to be active.

The distribution of earthquakes in Figures 13, 15, and 16 is biased by the station distribution (Figure 2) which allows detection and location of smaller events along the coast than offshore or further inland. The study area was divided into six west-northwest-east-southeast striking zones and the magnitude distribution was reviewed for each. While the distribution for the zone extending from the coast to about 100 km inland appeared to be complete for events of about coda magnitude 1.6 and larger, the magnitude level of completeness increased to about 2.4 for the most northerly and

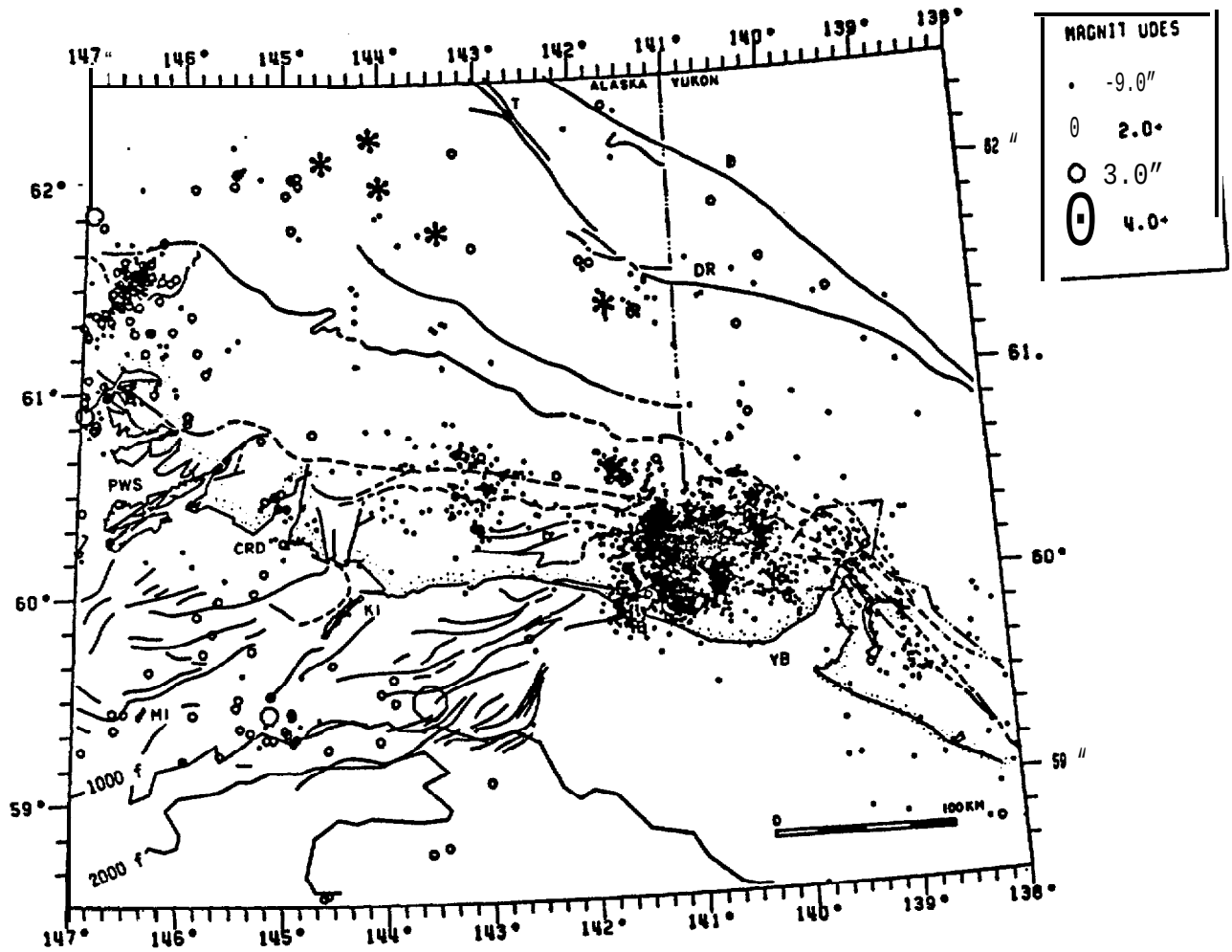

Figure 15a. Epicenter map of 3534 earthquakes located by the local seismograph network between October 1, 1979 and September 30, 1980. Labels same as Figure 6a.

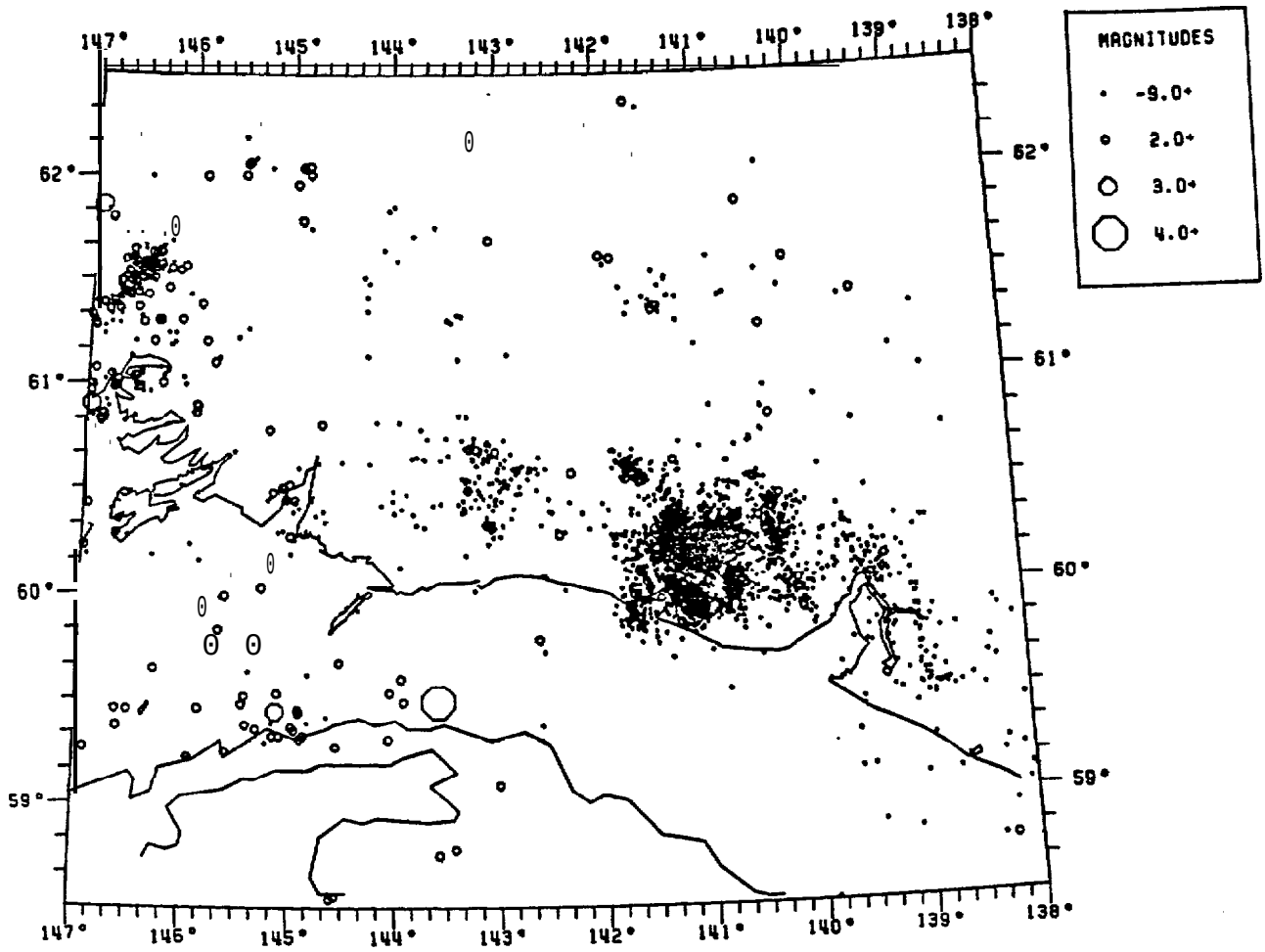

Figure 15b. October 1, 1979 through September 30, 1980 epicenters, as in Figure 15a.

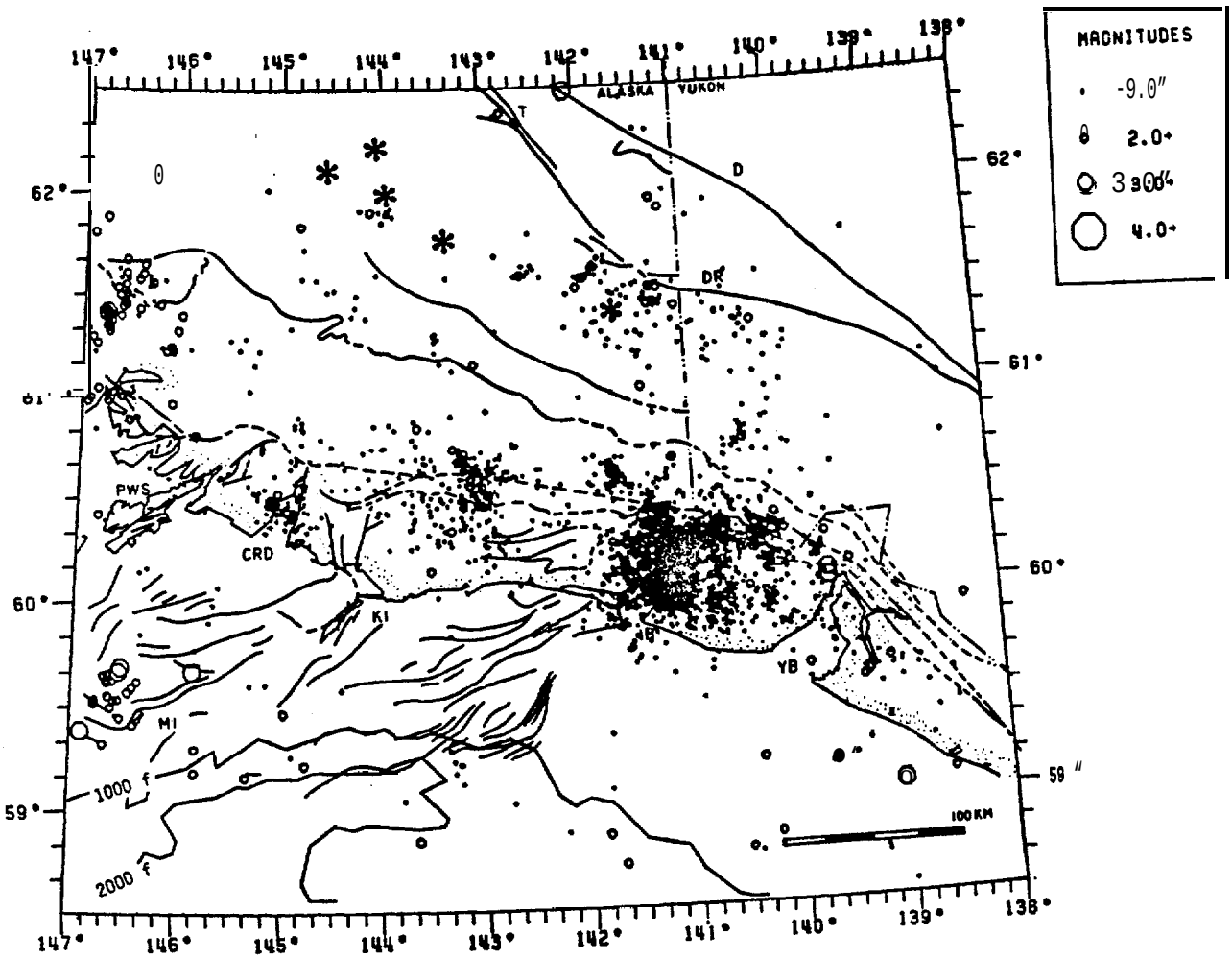

Figure 16a. Epicenter map of 3811 earthquakes located by the local seismograph network between October 1, 1980 and September 30, 1981. Labels same as **Figure** 6a.

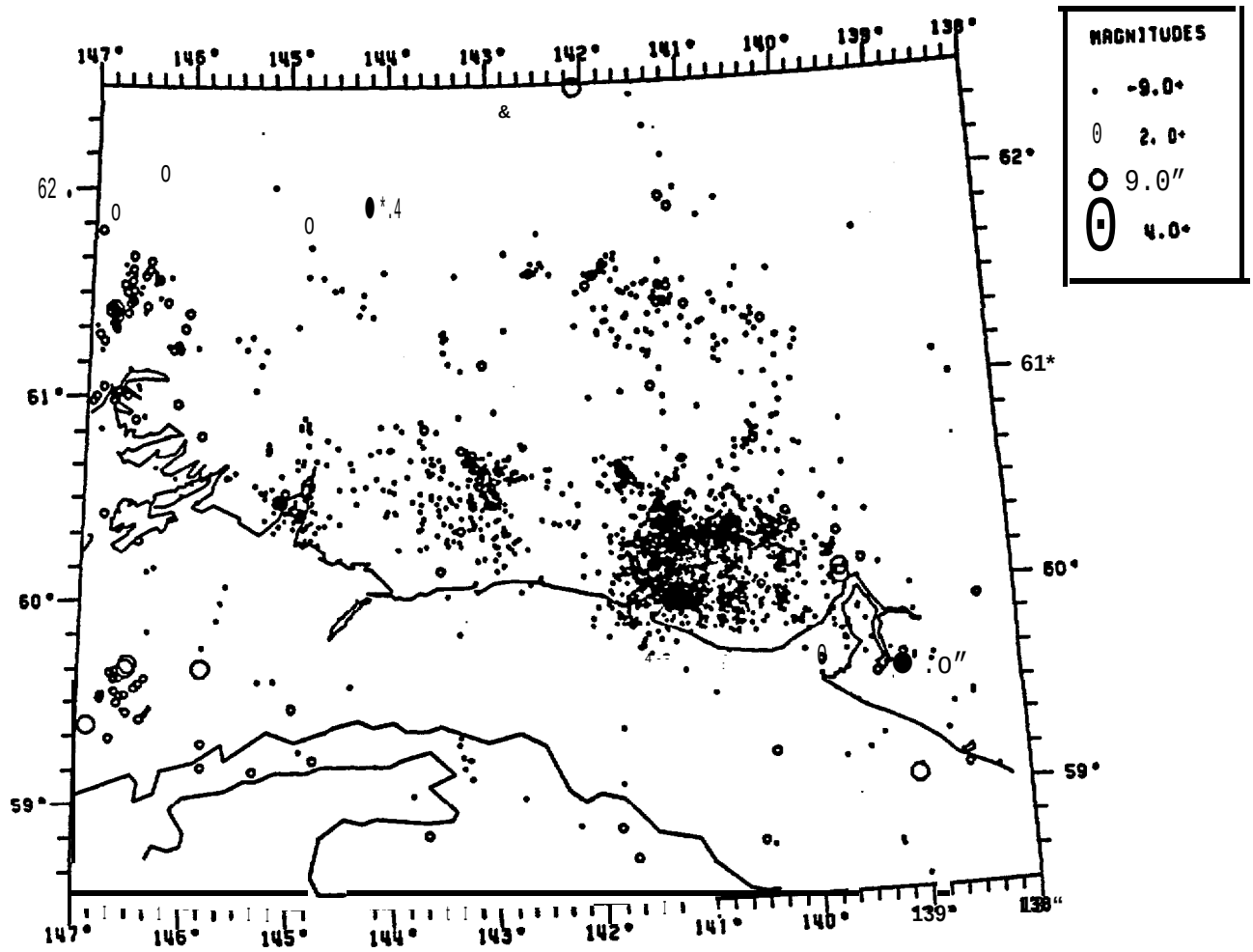

Figure 16b. October 1, 1980 through September 30, 1981 epicenters, as in Figure 16a.

southerly zones. Figure 17 shows the distribution of events with coda magnitude 2.4 and greater for October 1, 1974 through September 31, 1981. Although this figure is not complete in time, due to some gaps in processing, there should be little spatial bias in completeness caused by the station distribution. Some of the areas of high activity, such as near Waxen Ridge and the Copper River Delta, are no longer prominent when events below magnitude 2.4 are excluded, and the seismicity is seen to be much more uniformly spread throughout the region, both onshore and offshore, than in the previous figures (13-16). It is notable that the least active portion of the coast extends from the St. Elias aftershock zone to the Copper River Delta, approximately the same portion of coast identified as the Yakataga seismic gap.

Offshore, concentrations of activity have been identified south of Yakutat Bay (Figure 13) and in several areas west of about 142" 30' W longitude (Figures 13 through 16). The rates of activity in offshore areas vary considerably with time. For example, little activity has been observed south of Yakutat Bay since 1974 when a prominent swarm of activity occurred. Also, little activity has been observed near the Pamplona Ridge since the network was expanded in 1974, but this had been the site of a sequence of two magnitude 6 earthquakes in 1970 (Figure 10). It is notable that intermediate and larger earthquakes can occur in areas that exhibit relatively low rates of microearthquake activity. For example, a magnitude 5.2 m_b earthquake that occurred near 59°30' N, 143° 30' W in September, 1980 (Figure 15) was the largest event in that area in almost 10 years, but little activity had been located in the same area by the local network in the preceding six years.

C. Estimation of recurrence times for major earthquakes

One of the most critically needed and also most difficult tasks is estimation of the likelihood of major earthquakes, approximately magnitude 7 and larger, that have the potential for causing widespread damage and loss of life. A prerequisite is the understanding of the kinematics of the region including the identification of the major fault boundaries and the slip rate on each. A number of techniques can then be used to estimate the recurrence time for major events on each identified fault.

One possible technique would be to determine the constants A and b in the Gutenberg-Richter magnitude distribution

$$\log N = A - b M \qquad (4)$$

where N is the number of events per year with magnitudes greater than or equal to M. Typically data are not available for a long period of time so A and b must be determined on the basis of events with magnitudes between M_{min} and M_{max}, where M_{max} is 2 or more units smaller than the potentially damaging earthquakes of concern. The relationship is then extrapolated to determine the average recurrence time for major earthquakes. This method has the following drawbacks:

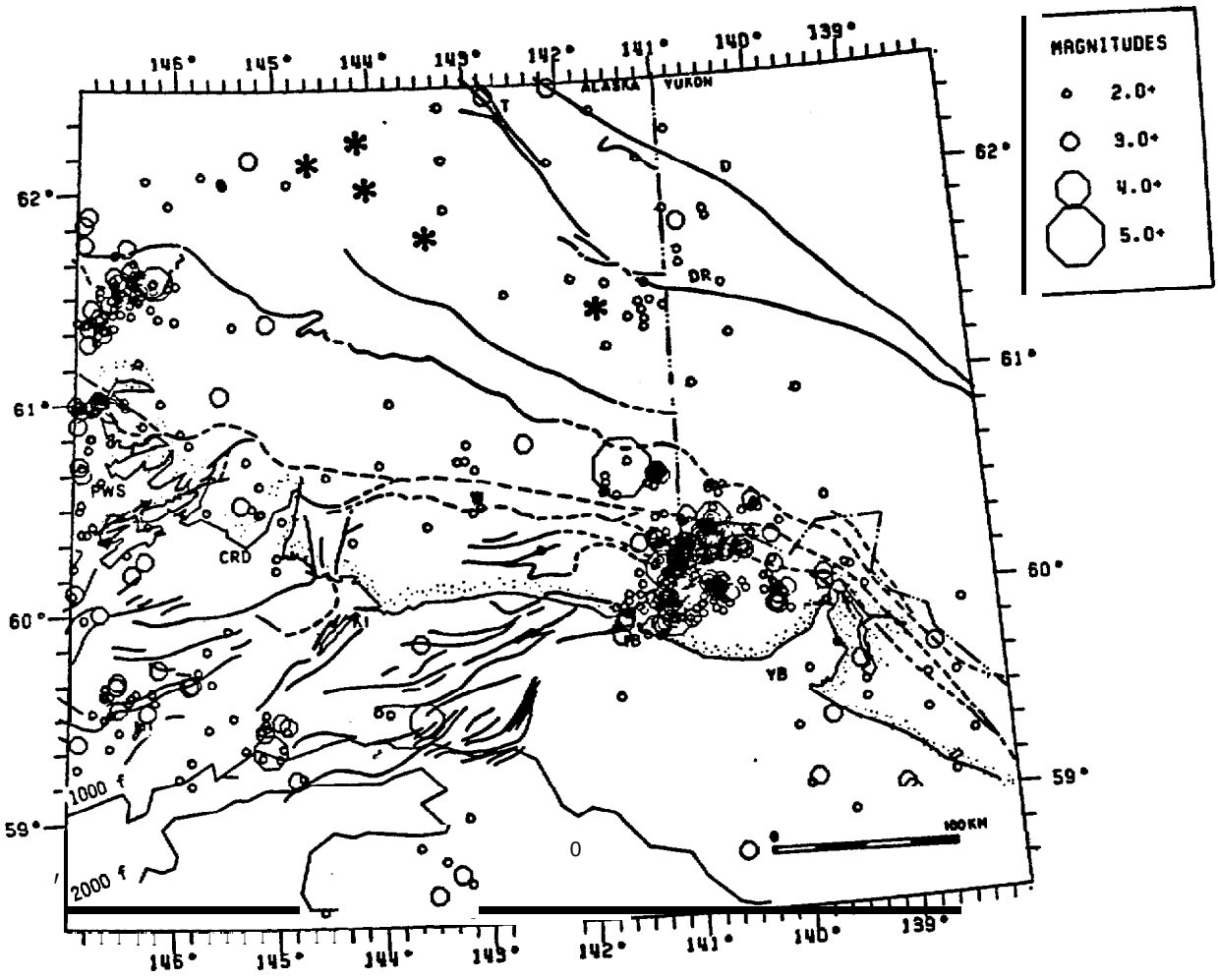

Figure 17a. Epicenter map of 643 earthquakes with coda magnitude **greater** than or equal to 2.4 located by the local seismograph network between October 1, 1974 and September 30, 1981. Labels same as Figure **6a.**

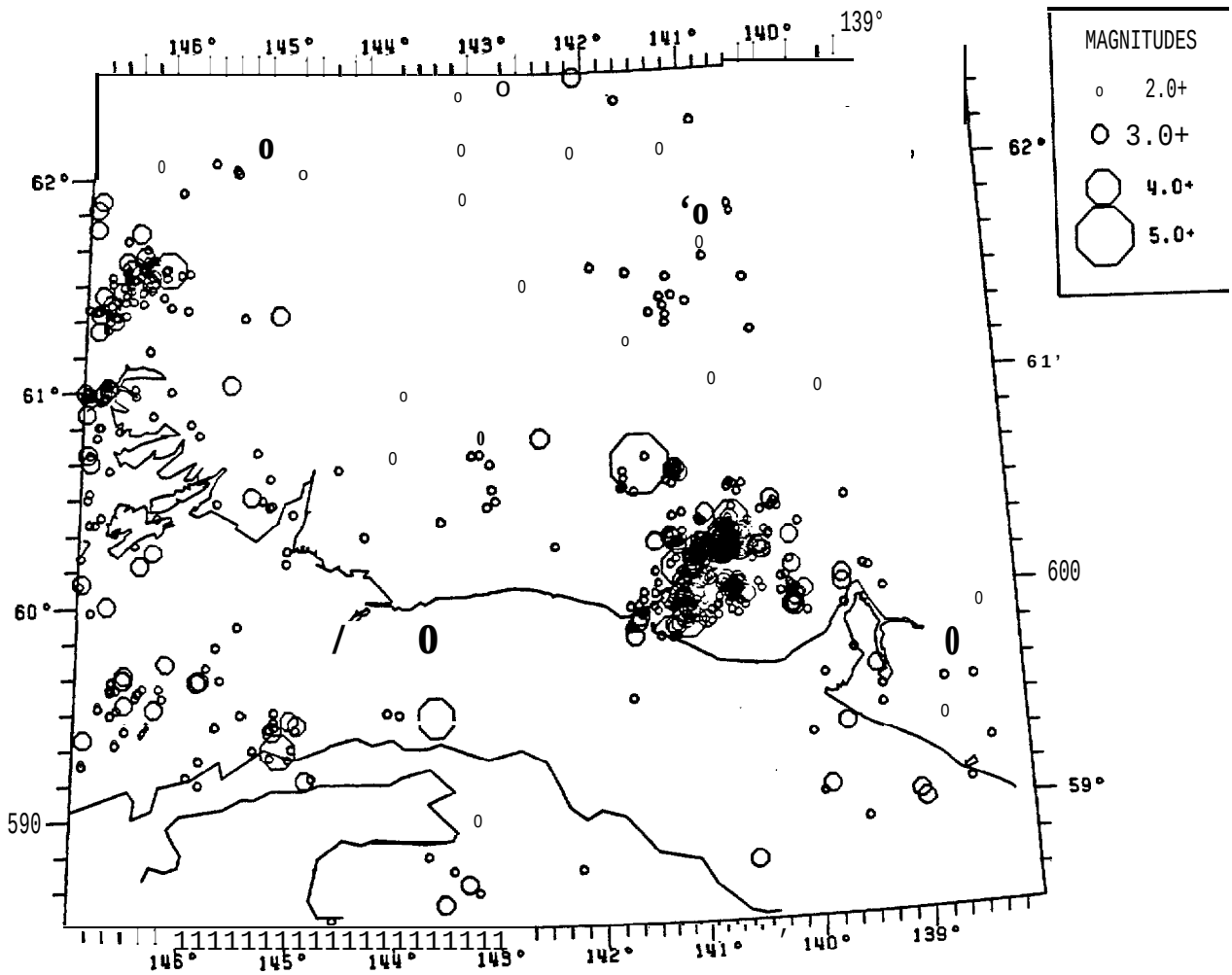

Figure 17b. October 1, 1974 through September 30, 1981 epicenters, as in Figure 17a.

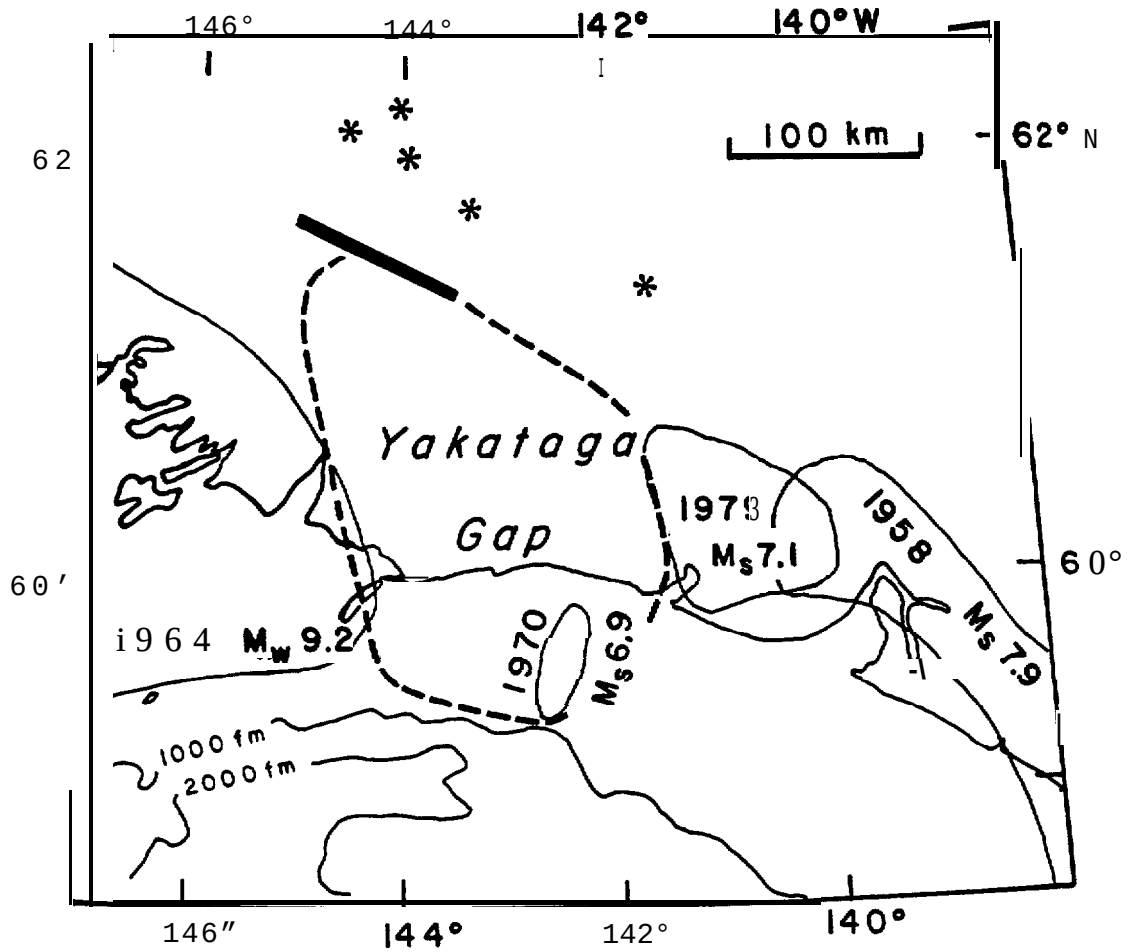

Figure 18. Principal rupture zones of **NEGOA** region and possible extent **of Yakataga** seismic gap (dashed). Approximate location of 40 km isobath of **Wrangell Benioff** zone given by heavy solid line.

1) The rate of activity may not be constant in time, so a short time interval may not be representative of the long-term average. Episodic behavior has been suggested by many authors (Tobin and Sykes, 1968; Kelleher, 1970; Sykes, 1971; Davies and House, 1979). This could lead to either over- or under-estimating the recurrence times for major events.

2) There is serious question as to the applicability of equation 4 to individual faults, even though the relationship holds well for global and regional scales (Richter, 1958; Anderson and Enrique, 1983). For an individual fault, the number of events near the maximum may be considerably higher than would be predicted from the extrapolation of equation 4 (Lahr, 1982).

An alternative procedure uses the slip rate, fault area and maximum stress drop to estimate the average recurrence-interval as a function of magnitude range (Molnar, 1979). This method has the advantage of not relying on a short interval of observations, but like the first technique it assumes that equation 4 is valid for individual faults, and also requires knowledge of the slip rate, fault area and maximum stress drop.

Considering the uncertainties in the proposed kinematic model for the eastern Gulf of Alaska, in the magnitude distribution for individual faults, and in the relative proportion of seismic versus aseismic slip, only an approximate estimate of recurrence times can be offered at this time. An estimate has been made simply by dividing the estimated slip for the largest expected earthquake by the average fault slip rate taken from the model. The estimated recurrence time will be too short to the extent that significant slip occurs aseismically or during smaller earthquakes, and too long to the extent that the estimated slip for the maximum event is too large. Estimates are given in Table 1 for the two principal seismic sources in the eastern Gulf of Alaska region.

SSG1ON:	BOUNDARIES	SLIP RATS (cm/yr)	ARSA (id)	DISPLACEMENT (c m) *	M_o (10^{29} dyne-cm)	M_w	RECURRENCE TINS (yr)
Underthrusting of Yakutat block and Pacific plate below Wrangell block.	Kayak Island, Pamplona zone, Icy Bay, 40 km depth of Benioff zone to north.	4.4	40000	640	1.8	8.8	145
Underthrusting of the Pacific plate below the Yakutat block	Transition zone, Fairweather fault, Pamplona zone.	0.4	22500	640	1.0	8.6	1,600

* The displacement, u, is estimated from

$$u = \frac{3 \Delta\sigma W}{4 \mu}$$ (Molnar, 1979)

Assuming: 1) maximum stress drop, $\Delta\sigma$, of 30 bars (3x 10^7 dyne cm-2), typical of the largest eventa (Kanamori and Anderson, 1975),
2) μ = 7 x 10^{11} dyne cm^{-1}, and
3) W, the down dip length, is about 200 km in each case.

Table 1. Estimated recurrence times for two principal seismic sources in the eastern Gulf of Alaska region.

D. Strong-motion recordings

From 1974 through 1981 funding was available from OCSEAP to help puchase and maintain Alaskan strong-motion instruments (see Figure 2). During this time interva strong-motion recordings were obtained from three earthquakes in the eastern Gulf of Alaska region. The 1979 St. Elias earthquake triggered 3 of the 6 accelerographs in operation within 250 km of the epicenter. In addition, digital accelerograph data were obtained at Valdez by the Alyeska Pipeline Service Company. The maximum horizontal acceleration recorded from the St. Elias earthquake was 0.16 g (1 g = 980 cm/sec^2) at Icy Bay (GYO), located 74 km from the epicenter.

Two earthquakes near Yakutat Bay triggered the nearest instrument at Bancas Point (BCP) in September 1981. Bancas Point is about 12 km from these events and recorded a maximum horizontal acceleration of 0.06 g. In each case, the accelerograph was triggered by the S-wave motion.

The preliminary strong-motion results are summarized in Table 2 below:

Table 2. Preliminary strong-motion results.

Date	EARTHQUAKE Time (UT)	Magnitude M_{coda}	m_b	M_s	Depth (km)	Recording Station	Epicentral Distance (km)	Max. Horiz. Ace. (g)
02/28/79	21:27			7.1	13	Munday Creek	69	0.06 (1)
						GYO	74	0.16 (2)
						CYT	75	No Trigger
						Yakutat	164	0.09 (2)
						Kayak Island	181	No Trigger
						Cordova	222	No Trigger
						Valdez	225	0.013 (3)
09/11/81	05:02	3.6	4.0		7	BCP	12	0.06 (4)
09/17/81	00:18	3.3	3.8		9	BCP	11	0.05 (4)

Source for accelerations:

(1) Based on data processed by Kinemetrics Inc. for Shell Oil Co.

(2) Porcella (1979). These records have been processed and are available in digi form from NOAA/NGDC, Boulder, Colorado 80303.

(3) Recorded digitally by Alyeska Pipeline Service Company (Personal communication R. C. Wahrmund, 1980).

(4) Personal communication, R. L. Porcella, 1982.

VII. CONCLUSIONS

The eastern Gulf of Alaska region is in a highly active tectonic region and will be subjected to earthquakes from five distinguishable seismic source regions:

1) Underthrusting of the Pacific plate below the Wrangell block northwest of the Aleutian megathrust. The 1964 Alaska earthquake (9.2 M_W) was of this type and ruptured from about Kayak Island (see Figure 9b) to southern Kodiak Island.

2) Underthrusting of the Yakutat block and the Pacific plate below the Wrangell block. This source region extends approximately 200 km northwest from the Pamplona zone. The February 1979 St. Elias earthquake (7.1 M_S) noted in Figures 1 and 5 was of this type. The Yakataga seismic gap, between Icy Bay and Kayak Island, is thought to be a likely site for a magnitude 8 or larger earthquake within the next two or three decades (McCann and others, 1980; Lahr and Plafker, 1980) .

3) Faulting along the northeast boundary of the Yakutat block. Typical of this would be the 1958 earthquake (7.9 M_S) which involved dextral strike-slip on the Fairweather fault. Also included would be the Yakutat Bay earthquake (8.4 M_S) of September 10, 1899 which involved complex thrust faulting with as much as 14 m of vertical displacement (Thatcher and Plafker, 1977)

4) Underthrusting of the Pacific plate below the Yakutat block. Although no historic great earthquake of this type is known to have occurred, it would not be prudent to exclude the possibility of one occurring in the future.

5) Moderate and large-size earthquakes ($5.5 < M_S < 8$) occurring anywhere within the Yakutat, St. Elias, and Wrangell blocks. Although the largest earthquakes, in categories 1 through 4, would account for nearly all of the plate motion, smaller events that could occur on smaller geologic structures, few of which are currently known, should also be taken into account.

VIII. NEEDS FOR FURTHER STUDY

Although substantial progress has been made towards understanding the current mode of tectonic deformation in the eastern Gulf of Alaska region, considerable additional research will be required to further develop and verify the current tentative model. Geologic work is essential for problems such as finding the source of the exotic Yakutat block and determining its structure, extent, and the timing of its collision with southern Alaska. Seismic studies, particularly those which provide good depth control for hypocenter determinations, will be useful in mapping the complex geometry of faults that are currently active, including both the main detachment thrust and secondary faults. Inversion of seismic data

from local earthquakes, teleseisms, and refraction shots for improved 3-D velocity structure will give direct insight into the structures present in this region as well as allow for more accurate earthquake locations. Continued direct measurements of crustal deformation and displacements by techniques including leveling (both level lines and tilt meters), trilateration, strainmeters and tide gauges will also provide important constraints on future tectonic models of the region.

IX. ACKNOWLEDGEMENTS

This report has benefited greatly from the thorough reviews of Robert A. Page and James N. Taggart. We are grateful for the contributions of the many people who assisted in this work, both in establishing and maintaining the seismic stations and in processing the data.

We thank Tom Sokoloski and the staff of the NOAA Alaska Tsunami Warning Center for their assistance in maintaining our recording equipment in Palmer, Alaska, as well as for making their seismic data available to us.

This study was supported jointly by the U.S. Geological Survey and by the National Oceanic and Atmospheric Administration, under which a multi-year program responding to needs of petroleum development of the Alaskan continental shelf is managed by the Outer Continental Shelf Environmental Assessment Program (OCSEAP) office.

X. REFERENCES

Anderson, J. G., and Luco, J. E., 1983, Consequences of slip rate constraints on earthquake occurrence relations: Bulletin of the Seismological Society of America, v. 73, no. 2, p. 471-496.

Beikman, H. M., 1978, Preliminary geologic-map of Alaska: U.S. Geological Survey Map, 1:2,500,000.

Bruns, T. R., 1979, Late cenozoic structure of the continental margin, northern Gulf of Alaska: in Sisson, Alexander, cd., Proceedings, Alaska Geological Society Symposium, 6th: Anchorage, 1977, Alaska Geological Society, p. 11-130.

Buland, Ray and Taggart, James, 1981, A Mantle wave magnitude for the St. Elias, Alaska, earthquake of 28 February 1979: Bulletin of the Seismological Society of America, v. 71, p. 1143-1159.

Clague, J. J., 1979, The Denali fault system in southwest Yukon Territory--a geologic hazard: in Current Research, Part A, Geological Survey of Canada, Paper 79-3A, p. 169-178.

Davies, J. N., and House, Leigh, 1979, Aleutian subduction zone seismicity, volcano-trench separation and their relation to great thrust-type earthquakes: Journal of Geophysical Research, v. 84, p. 4583-4591.

Deininger, J. W., Jr., 1972, Petrology of the Wrangell volcanoes near Nabesna, Alaska: University of Alaska, M.S. in Geology, 66 p.

Eaton, J. P., O'Neill, M. E., and Murdock, J. N., 1970, Aftershocks of the 1966 Parkfield-Cholame, California, earthquake: a detailed study: Bulletin of the Seismological Society of America, v. 60, p. 1151-1197.

Gawthrop W., Page, R. A., Reichle, M., and Jones, A., 1973, The southeast Alaska earthquake of July 1973: EOS, Transactions of the American Geophysical Union, v. 54, p. 1136.

Gutenberg, Beno, and Richter, C. F., 1954, Seismicity of the Earth, 2nd cd., Princeton University Press, Princeton, N. J.

King, P. B., 1969, Tectonic map of North America: Denver, Colorado, U. S. Geological Survey, 2 sheets.

Hastie, L. M., and Savage, J. C., 1970, A dislocation model for the 1964 Alaska earthquake: Bulletin of the Seismological Society of America, v. 60, p. 1389-1392.

Homer, R. B., In press, Seismicity in the St. Elias region of northwestern Canada and southern Alaska: Submitted to: Bulletin of the Seismological Society of America.

Kelleher, John, 1970, Space-time seismicity of the Alaskan-Aleutian seismic zone: Journal of Geophysical Research, v. 75, p. 5745-5746.

Lahr, J. C., 1975, Detailed seismic investigation of Pacific-North American plate interaction in southern Alaska, Ph.D. dissertation, Columbia University, 141 p.

Lahr, J. C., and Plafker, George, 1980, Holocene Pacific-North American plate interaction in southern Alaska: Implications for the Yakataga seismic gap: Geology, v. 8, p. 483-486,

Lahr, J. C., Plafker, George, Stephens, C. D., Fogleman, K. A., and Blackford, M. E., 1979, Interim report on the St. Elias, Alaska, earthquake of 28 February 1979: U.S. Geological Survey Open-File Report 79-670, 35 p.

Lahr, J. C., and Stephens, C. D. 1982, Alaska seismic zone: Possible example of non-linear magnitude distribution for faults: Earthquake Notes, Eastern Section, Seismological Society of America, v. S3, p. 66.

Lee, W. H. K., Bennett, R. E. and Meagher, K. L., 1972, A method of estimating magnitude of local earthquakes from signal duration: U. S. Geological Survey Open-File Report, 28 p.

Lee, W. H. K., and Lahr, J. C., 1972, HYPO71: a computer program for determining hypocenter, magnitude, and first motion pattern of local earthquakes: U. S. Geological Survey Open-File Report, 100 p.

MacKevett, E. M., Jr., 1978, Geologic map of the McCarthy Quadrangle, Alaska: U. S. Geological Survey Miscellaneous Geological Investigation Map 1-1032.

McCann, W. R., Nishenko, S. P., Sykes, L. R., and Krause, J., 1979, Seismic gaps and plate tectonics: seismic potential for major boundaries: Pure and Applied Geophysics, v. 117, p. 1082-1147.

McCann, W. R., Perez, O. J., and Sykes, L. R., 1980, Yakataga seismic gap, southern Alaska: seismic history and earthquake potential: Science, V. 207, p. 1309-1314.

Minster, J. and-Jordan, T., 1978, Present-day plate motions: Journal of Geophysical Research, v. 83, p. 5331-5354.

Molnar, Peter. 1979, Earthquake recurrence intervals and plate tectonics: Bulletin of the Seismological Society of America, v. 69, p. 115-133.

Page, R. A., 1968, Aftershocks and microaftershocks of the great Alaska earthquake of 1964: Bulletin of the Seismological Society of America, V. 58, p. 1131-1168.

Page, R. A., 1975, Evaluation of seismicity and earthquake shaking at off-shore cites, in Offshore Technology Conference, 7th, Houston, Texas, Proceedings, 3, p. 179-190.

Plafker, George, 1969, Tectonics of the March 27, 1964, Alaska earthquake: U. S. Geological Survey Professional Paper 543-1, 74 p.

Plafker, George, Hudson, T., Bruns, T., and Ruben, M., 1978, Late Quarternary offsets along the Fairweather fault and crustal plate interactions in southern Alaska: Canadian Journal of Earth Sciences, V. 15, p. 805-816.

Plafker, George, and Mayo, L. R., 1965, Tectonic deformation, subaqueous slides and destructive waves associated with the Alaskan March 27, 1964 earthquake: An interim geologic evaluation: U. S. Geological Survey Open-File Report, 19 p.

Porcella, R. L., 1979, Recent strong-motion records, in U. S. Geological Survey Circular 818-A, pl, Seismic engineering program report January - April 1979.

Richter, C. F., 1958: Elementary Seismology, W. H. Freeman and Company, San Francisco, 768 p.

Stephens, C. D., Astrue, M. C., Pelton, J. R., Fogleman, K. A., Page, R. A., Lahr, J. C., Allan, M. A., and Helton, S. M., 1982, Catalog of earthquakes in southern Alaska, April-June, 1978, U. S. Geological Survey Open-File Report 82-488, 36 p.

Stephens, C. D., Fogleman, K. A., Lahr, J. C. and Page, R. A., 1983, Evidence for a north-northeast dipping Benioff zone south of the Wrangell volcanoes, southern Alaska: (submitted to EOS, Transactions of the American Geophysical Union).

Stephens, C. D., Lahr, J. C, Fogleman, K. A., and Homer, R. B., 1980, The St. Elias, Alaska, earthquake of February 28, 1979: Regional recording of aftershocks and short-term, pre-earthquake seismicity: Bulletin of the Seismological Soceity of America, v. 70, p. 1607-1633.

StOver, C. W., Reagor, B. G., and Wetmiller, R. J., 1980, Intensities and isoseismal map for the St. Elias earthquake of February 28, 1979: Bulletin of the Seismological Society of America, v. 70, p. 1635-1649.

Sykes, L. R., 1971, Aftershock zones of great earthquakes, seismicity gaps, and earthquake prediction for Alaska and the Aleutians: Journal of Geophysical Research, v. 76, p. 8021-8041.

Tarr, R. S., and Martin, L., 1912, The earthquakes at Yakutat Bay, Alaska, in September, 1899: U. S. Geological Survey Professional Paper 69, 135 p.

Thatcher, W., and Plafker, George, 1977, The 1899 Yakutat Bay, Alaska earthquake: IASPEI/IAVCEI Assembly Abstracts with Programs, p. 54.

Tobin, D. G., and Sykes, L. R., 1966, Relationship of hypocenters of earthquakes to the geology of Alaska: Journal of" Geophysical Research, V. 71, p. 1659-1667.

Tobin, D. E. and Sykes, L. R., 1968, Seismicity and tectonics of the northeast Pacific Ocean: Journal of Geophysical Research, v. 73, p. 3821-3845.

Tocher, D., 1960, The Alaska earthquake of July 10, 1958: Movement on the Fairweather fault and field investigations of southern epicentral regions: Bulletin of the Seismological Society of America, v. 50, p. 267-292.